

https://dspace.org/

Design of a transdermal anti-psoriatic hydrogel drug delivery system for the treatment of psoriasis vulgaris

Mohlomi, Matsoso Lauwrence

2021

https://hdl.handle.net/10539/33499

Downloaded from a DSpace repository. https://dspace.org/

DESIGN OF A TRANSDERMAL ANTI-PSORIATIC HYDROGEL DRUG DELIVERY SYSTEM FOR THE TREATMENT OF PSORIASIS VULGARIS

MATSOSO LAUWRENCE MOHLOMI

A Dissertation submitted to the Faculty of Health Sciences, University of the Witwatersrand, in fulfilment of the partial requirements for the degree of Master of Science in Medicine with specialization in Pharmaceutical Affairs.

Supervisors:

Professor Pierre Kondiah
Professor Yahya E. Choonara
Doctor Sipho Mdanda

University of the Witwatersrand, Department of Pharmacy and Pharmacology, Johannesburg, South Africa

Johannesburg, 08 October 2021

DECLARATION

I, Matsoso Lauwrence Mohlomi, declare that this Dissertation is my own work. It is being submitted for the degree of Master of Science in Medicine in the field of Pharmaceutical Affairs in the Faculty of Health Sciences as a research component at the University of the Witwatersrand, Johannesburg. It has not been submitted before for any degree or examination at this or any other University.



……

Signature

On this ……08……day of ……October…… 2021

DEDICATION

This dissertation is dedicated to my partner and source of strength, joy, and comfort, and counselor Theophelus Mahlangu – this one is for us.

ACKNOWLEDGEMENTS

I would first like to take this opportunity to give my heartfelt gratitude to the School of Therapeutic Sciences for the granting me the opportunity to further my academic studies and fulfil my academic endeavours. My appreciation goes out to my friends and colleagues for making the journey enjoyable!

To Dr Jonathan Monwabisi Pantshwa, Dr Phil Ubanako, Dr Sipho Mdanda, Professor Pierre Kondiah, and Professor Yahya E. Choonara thank you for your incredible guidance, patience, and mentorship.

To the National Research Fund, Professor Kondiah's Thuthuka grant – deep thank you for funding this research project.

My sincerest thank you to my parents and my sibling for your love and support, and most of all for believing in me and in my dreams. All of this is made possible by you.

To MMS Holdings management, thank you for the support and flexibility to allow me to complete my research while working full time, and to Esta and Allison for your continued concern and care.

I would also like to extend gratitude to the support and technical staff at the Pharmacy and Pharmacology department - thank you for all your assistance and support.

ABSTRACT

Psoriasis vulgaris (PV) is a chronic disease. Hydrocortisone (HCT) is currently utilized as a treatment however, it is associated with undesirable side effects. The aim of this study was to create a thermos-responsive nano-hydrogel delivery system. HCT-loaded Sorbitan monostearate (SMS)-polycaprolactone (PCL) nanoparticles encapsulated with thermo-responsive hydrogel carboxymethyl cellulose (CMC) were synthesized applying interfacial polymer deposition method following solvent displacement. Nanoparticles' properties were evaluated employing Differential Scanning Colorimetry, Thermogravimetric Analysis, Fourier Transform Infrared Spectroscopy, Scanning Electron Microscopy, Zeta sizer, Ultraviolet/Visual spectroscopy and cytotoxicity testing. The nanoparticle sizes were 110.5 nm with polydispersity index of 0.15 and the zeta potential of -58.7 mV. The drug entrapment efficacy of 76% was attained by the HCT-loaded SMS-PCL nanoparticles and in vitro drug release profiles showed continued drug release over a period of 24 hrs. Keratinocyte skin cells were treated HCT-loaded SMS-PCL nanoparticles encapsulated with CMC, the results indicated that the synthesized drug delivery system was less toxic to the keratinocyte cells compared to HCT. The combined trials and results from the formulation of HCT-loaded SMS-PCL nanoparticles encapsulated CMC, showed evidence that this hydrogel can be utilized as potential invaluable formulation for transdermal drug delivery of HCT with improved efficacy and patient conformity.

Keywords: Hydrogels, Polymers, Drug delivery, Psoriasis vulgaris

TABLE OF CONTENTS

DECLARATION ---- I
DEDICATION ---- II
ACKNOWLEDGEMENTS ---- III
ABSTRACT ---- IV
TABLE OF CONTENTS ---- V
LIST OF FIGURES ---- VII
LIST OF TABLES ---- IX
LIST OF EQUATIONS ---- X
LIST OF ABBREVIATIONS ---- XI
CHAPTER 1. BACKGROUND AND INTRODUCTION ---- 1
1.1 INTRODUCTION ---- 1
1.2 STUDY RATIONALE AND MOTIVATION ---- 2
1.3 AIM AND OBJECTIVES ---- 4
1.4 OVERVIEW OF THIS DISSERTATION ---- 5
CHAPTER 2. A REVIEW OF LITERATURE ON THERMO-RESPONSIVE HYDROGEL SYSTEMS USED IN THE TREATMENT OF INFLAMMATORY SKIN DISEASES ---- 7
2.1 INTRODUCTION ---- 7
2.1.1 Review of Psoriasis and Current Therapeutic Interventions ---- 7
2.2 TOPICAL DRUG DELIVERY ---- 13
2.2.1 Anatomy of the skin ---- 13
2.2.2 Drug Delivery across the skin ---- 14
2.2.3 Hydrogels as potential therapeutic agents ---- 15
2.3 HYDROGELS ---- 16
2.3.1 Thermo-responsive Hydrogels ---- 16
2.3.1.1 Natural polymers ---- 19
2.3.1.2 Synthetic polymers ---- 20
2.4 CORTICOSTEROIDS ---- 21
2.4.1 Pharmacokinetics ---- 23
2.4.2 Pharmacodynamics ---- 24
2.5 TREATMENT OF PSORIASIS: RECENT TOPICAL APPLICATIONS ---- 24
2.5.1 Topical Creams ---- 24
2.5.2 Topical Aerosol Foams ---- 26
2.5.3 Hydrogels for Topical Applications ---- 27
2.6 CONCLUDING REMARKS ---- 28
CHAPTER 3. DESIGN AND SYNTHESIS OF A TRANSDERMAL ANTI-PSORIATIC HYDROGEL FOR THE TREATMENT OF PSORIASIS VULGARIS ---- 29
3.1 INTRODUCTION ---- 29
3.2 MATERIALS AND METHODS ---- 30
3.2.1 Materials and Equipment ---- 30
3.2.2 Spectrophotometric Determination of λ_{max} of HCT and Calibration Curve ---- 31
3.2.3 Synthesis of the SMC-PCL Nanoparticle Carrier System ---- 32
3.2.4 Physical Assessment of the SMS-PCL Nanoparticles in Terms of Size, Stability, and Charge Distribution ---- 33
3.2.5 Determination of the Drug Entrapment Efficacy of HCT within the SMS-PCL Nanoparticles ---- 33

3.2.6 Chemical Evaluation Undertaken on the SMS-PCL nanoparticles, HCT, and HCT-loaded nanoparticles ---- *34*
3.2.7 Thermal Transition Evaluation of the SMS-PCL nanoparticles, HCT, and HCT-loaded nanoparticles ---- *34*
3.2.8 Thermal Evaluation of the SMS-PCL nanoparticles, HCT, HCT-loaded nanoparticles ---- *34*
3.2.9 Synthesis and Evaluation of the CMC Hydrogel System ---- *35*
3.2.10 In vitro Drug Release Undertaken on the SMS-PCL nanoparticles, as well as the Loaded CMC Hydrogel ---- *35*
3.2.11 Analysis of the Surface Morphology of the HCT-loaded Nanoparticles Using SEM ---- *36*
3.2.12 In vitro Cytotoxicity ---- *36*
3.2.12.1 Keratinocytes Culture Employing HaCaT Cell Lines ---- 36
3.2.12.2 Cell Morphology and Cell Count ---- 37
3.2.12.3 Standard Drug Preparation ---- 37
3.2.12.4 *In vitro* Cytotoxicity Assay Preparations ---- 37
3.2.12.5 MTT Cytotoxicity Assay to Determine the Safety and Tolerability of the HCT-loaded CMC Hydrogel ---- 38
3.2.12.6 Light Microscopy Analysis to Evaluate Internalization of the Therapeutic Compounds Within the HaCaT Cells ---- 39
3.3 RESULTS AND DISCUSSION ---- 40
3.3.1 Spectrophotometric Analysis Undertaken to Determine λ_{max} of HCT and Calibration Curve ---- *40*
3.3.2 Physical Assessment of the SMS-PCL Nanoparticles in Terms of Size, Stability, Charge Distribution, And Drug Entrapment ---- *41*
3.3.3 Chemical Evaluation Undertaken on the SMS-PCL nanoparticles, HCT, and HCT-loaded nanoparticles ---- *42*
3.3.4 Thermal Transition Evaluation of the SMS-PCL nanoparticles, HCT, and HCT-loaded nanoparticles ---- *43*
3.3.5 Thermal Evaluation of the SMS-PCL nanoparticles, HCT, HCT-loaded nanoparticles ---- *44*
3.3.6 Evaluation of the CMC Hydrogel System for Sol-Gel Transition Temperature ---- *46*
3.3.7 In vitro Drug Release Undertaken on the SMS-PCL nanoparticles, as well as the Loaded CMC Hydrogel ---- *46*
3.3.8 Analysis of the Surface Morphology of the HCT-loaded Nanoparticles Using SEM ---- *47*
3.3.9 In vitro Cytotoxicity ---- *53*
CHAPTER 4. CONCLUSION AND FUTURE RECOMMENDATIONS ---- 57
CHAPTER 5. REFERENCES ---- 58

LIST OF FIGURES

Figure 1.1 Schematic representation of the thermo-responsive CMC hydrogel. The figure illustrates the HCT-loaded SMS-PCL nanoparticle delivery system and its release to the skin cells at approximately 37 ºC (Image from Álvarez-Paino *et a*l., 2017 with modifications). 4
Figure 2.1 Clinical Presentation of Psoriasis. The above figure shows different classifications of psoriasis. Figure 2.1(a) shows Psoriasis vulgaris, (b) Pustular psoriasis, (c) Guttate psoriasis, (d) Inverse psoriasis, and (e) Erythrodermic psoriasis. (Images used with permission from Rendon and Schakel, 2019). 8
Figure 2.2 Effects of Psoriasis. In this figure, the effects of psoriasis are shown from the skin, systemic effects, secondary diseases (cardiovascular disease (CVD) and psychiatric reactions), to the effects on the overall quality of life (Qol) and burden of disease (open source image obtained from WHO, 2016). 9
Figure 2.3 Treatment of mild, moderate, and severe psoriasis. *UVB = ultraviolet B-rays; PUVA = psoralen and ultraviolet A (Image adapted from Raboobee *et al*., 2010). 11
Figure 2.4 Anatomy of the Skin. The 3D figure shows the distinct skin layers. The outer epidermis is a keratinized superficial layer of the skin, deep to that is the dermis, a highly vascularized layer (Image obtained from Marieb and Hoen, 2012). 14
Figure 2.5 Illustration of UCST and LCST in thermo-responsive hydrogels. The figure shows the sol-gel transition of hydrogels when a specific temperature (CST) is reached (adapted from Altomare et al., 2018). 17
Figure 2.6 Schematic representation of the thermo-responsive hydrogel system. This figure shows the process of drug release when LCST of the hydrogel is reached. (Image used with permission from Lale and Koul, 2018). 18
Figure 2.7 Structure of Mometasone furoate (MF). 21
Figure 2.8 Structure of Hydrocortisone. 22
Figure 2.9 Structure of Dexamethasone. 22
Figure 3.1 Illustration of the microemulsion method. The figure demonstrates loading of HCT into a micellar structure (SMS-PCL nanoparticle) for loading into the hydrogel (Image obtained from Güngör et al. (2015) with modification). 32
Figure 3.2: Schematic representation of the synthesis process for the HCT-loaded SMS-PCL nanoparticles. 33
Figure 3.3 Calibration curve of HCT. 40
Figure 3.4 Nanoparticle size of (a) HCT-loaded and (b) SMS-PCL Blank nanoparticles 41
Figure 3.5 FTIR Spectra of the SMS-PCL Blank polymers, HCT drug (pure), and HCT-loaded nanoparticles. 42
Figure 3.6 DSC of HCT, SMS-PCL Blank, and HCT-loaded nanoparticles. 44
Figure 3.7 TGA thermograms of (a) HCT, (b) SMS-PCL blank, and (c) HCT-loaded nanoparticles. 45
Figure 3.8 SEM micrograph of the HCT-loaded SMS-PCL nanoparticles confirming their polymeric structure. 47
Figure 3.9 HCT release profiles from SMS-PCL nanoparticles and CMC hydrogel at simulated PV skin pH (pH 5.2) at 37 ºC over a period of 24 Hrs. 52
Figure 3.10 HCT release profiles from SMS-PCL nanoparticles and CMC hydrogel at simulated normal skin pH (pH 5.9) at 37 ºC over a period of 24 Hrs. 52
Figure 3.11 HaCaT Cell Viability (%) following treatment after 24 hours. The graph shows cell viability following MTT Assay of the treated cells against the controls. 53

Figure 3.12 HaCaT Cell Viability (%) following treatment after 48 hours. The graph shows cell viability following MTT Assay of the treated cells against the controls. 54
Figure 3.13 Light microscopy images of the (a) Plain Hydrogel, (b) HCT-Loaded hydrogel, (c) Pure HCT, (d) HCT-loaded nanoparticles, (e) Blank nanoparticles, (f) 5-FU, (g) Untreated cells, and (h) DMSO control after 48 hours treatment. 56

LIST OF TABLES

Table 2-1 Treatment Adherence, Satisfaction, and Preference in Psoriasis. 12
Table 2-2 Summary of widely studied polymers. The CST is provided for each respective polymer. 18
Table 2-3 Various Corticosteroid Formulations and Their Respective Trade Names. 22
Table 3-1 HCT Drug Release Profiles at pH 5.2 48
Table 3-2 HCT Drug Release Profiles at pH 5.9 50

LIST OF EQUATIONS

Equation 1 Drug Entrapment Efficacy (DEE) calculation of HCT within the SMS-PCL nanoparticles 34
Equation 2 Calculation of mass of HCT released from the SMS-PCL nanoparticles as well as SMS-PCL nanoparticles encapsulated within the CMC hydrogel 36
Equation 3 Calculation of number of viable cells 37
Equation 4 Cell viability calculation following MTT Assay 38

LIST OF ABBREVIATIONS

ATR	Attenuated total reflection
BM	Bethamethasone
BSA	Body surface area
Cal/BD	Calipotriol and betametasone dipropionate
CMC	Carboxymethyl cellulose
CST	Critical Solution Temperature
CVD	Cardiovascular disease
DEE	Drug Entrapment Efficacy
DEX	Dexamethasone
DMEM	Dulbecco's Modified Eagle's Medium
DMSO	Dimethyl sulfoxide
DSC	Differential Scanning Colorimetry
FBS	Foetal Bovine Serum
FTIR	Fourier Transform Infrared Spectroscopy
5-FU	5-Flourouracil
HCl	Hydrochloric acid
HCT	Hydrocortisone
HPA axis	Hypothalamus-Pituitary-Adrenal gland axis
HPC	Hydroxypropyl cellulose
HPMC	Hydroxypropylmethyl cellulose
IBS	Irritable bowel syndrome

IL	Interleukin
IR	Infrared
LA-Cer	Linoleic acid-Ceramides
LCST	Lower critical solution temperature
MF	Mometasone Furoate
MTT	Dimethylimidazole diphenyl tetrazolium bromide
MTX	Methotrexate
MW	Molecular weight
NaOH	Sodium hydroxide
NLC	Nanostructure lipid carriers
PASI	Psoriasis Area and Severity Index
PBS	Phosphate Buffered Saline
PCL	Polycaprolactone
PEG	Polyethylene glycol
PEOx	Poly(2-ethyl-2-oxazoline)
PiPOx	Poly(2-isopropyl-2-oxazoline)
PMOx	Poly(2-methyl-2-oxazoline)
pNIPAAm	Poly(N-isopropyl acrylamide)
PPG	Polypropylene glycol
PTT	Phase Transition Temperature
PUVA	Psoralen and ultraviolet A
PV	Psoriasis Vulgaris
P407	Poloxamer 407
SD	Standard Deviation

SEM	Scanning Electron Microsopy
SF	Silk fibroin
SGTT	Sol-gel transition temperature
SLN	Solid lipid nanoparticles
SMS	Sorbitan monostearate (Span60)
TAZ	Tazarotene
TGA	Thermogravimetric analysis
TNF	Tumour necrosis factor
TSQM	Treatment Satisfaction Questionnaire for Medication
Tween 80	Polysorbate 80
UCST	Lower critical solution temperature
UV/Vis	Ultraviolet/Visual
UVB	Ultraviolet B-ray
WHO	World Health Organization

CHAPTER 1. BACKGROUND AND INTRODUCTION

1.1 Introduction

Inflammatory skin conditions are a major public health concern ranking among the highest non-communicable diseases in the world (WHO, 2021). Globally, the prevalence of Psoriasis ranges between 2% to 5% of the population (Grozdev and Korman, 2021; Rocha *et al*., 2021) with increasing prevalence trends observed annually, thus adding on to the global burden of disease (Iskandar *et al*., 2021). The most common form of Psoriasis is the plaque-type Psoriasis Vulgaris (PV) – a disfiguring and incurable disease characterized by hyperproliferation of skin cells (Afonina *et al*., 2021; Limón *et al.*, 2019). Clinically, PV presents with red well-defined scaly plaque, pruritus (itching), erythema, oedema, fatigue, and burning (Menter and Ryan, 2017). This disease is also associated with a number of secondary illnesses including psoriatic arthritis, metabolic syndrome, and depression and anxiety (Maqbool *et al.*, 2021; Pannu *et al.*, 2021; Caso *et al*., 2020). The combination of multiple causes and associated secondary diseases of PV make it challenging to treat.

Current therapeutic interventions of this disease include corticosteroids, immune suppressants (calcineurin inhibitors), antihistamines, and antimicrobials, prescribed in the form of topical creams, ointments, and lotions (Steinhoff *et al.*, 2020). South African treatment guidelines state topical corticosteroids as standard care for the treatment of this disease (Jacobs and Kgokolo, 2020). Hydrocortisone, methylprednisolone acetonate, mometasone furoate, betamethasone valerate, and dexamethasone are some of corticosteroids commonly utilized (Del Rosso, 2020). Other therapeutic strategies include phototherapy and systemic therapy with methotrexate, active biological compounds, ciclosporin, and acitretin (Steinhoff *et al*., 2020). These drugs show efficacy as therapeutic agents against PV, however, they are associated with multiple undesirable adverse side effects. Furthermore, other factors contributing to the limitations of therapy include adherence to treatment by patients, cost, availability of medicines, and lack of knowledge about the pathogenesis of the diseases (Gold *et al.*, 2021; Svenden *et al.*, 2020). Thus, novel and improved efficacious treatment strategies are required.

There is a growing interest in the use of hydrogels as a method of topical drug delivery (Wollina *et al.*, 2019). In contrast to conventional therapy, hydrogels as topical drug delivery systems have several advantages including, improved patient's quality of life, sustained drug release, and drug adsorbed by surmounting the skin barrier. (Kumar, R. *et al., 2021*). Thermo-responsive hydrogels are hydrogels that respond to temperature as a stimulus (de Oliveira e*t al.*, 2021). Thermo-responsive hydrogels synthesised from natural polymers are more advantageous as they are biocompatible and biodegradable as compared to the synthetic polymers (Atanasova *et al*., 2021). Wang and colleagues studied the double network Poloxamer 407 (P407) and Carboxymethyl cellulose (CMCs) hydrogel combination for the treatment of Atopic dermatitis (an inflammatory skin condition) (Wang *et al.*, 2016). In this study, they found that the P407 hydrogel reinforced with CMCs yielded positive results. This hydrogel was able to release the model drug at temperatures near to physiological temperature into localised site of the diseases (Wang *et al.*, 2016).

The purpose of this study was to synthesise hydrocortisone (HCT) loaded (Sorbitan monostearate/SMS)-polycaprolactone (PCL) nanoparticles encapsulated with Carboxymethyl cellulose (CMC) hydrogel which is responsive to temperature (body temperature 37 ºC), pH (skin pH ~5.2) for improved transdermal treatment of PV. HCT was employed as a model corticosteroid drug since it is clinically utilized for psoriasis treatment. The SMS polymer has been demonstrated to have high entrapment efficiency and stability, thus ideal topical drug delivery system. The formulated hydrogel was then subjected to *in vitro* evaluation and cytotoxicity assay.

1.2 Study Rationale and Motivation

The epidermal tissue hyperplasia considerably affects the permeability of active drugs across the skin, thus making it challenging for PV to be treated (Armstrong and Read, 2020). Current conventional corticosteroid therapy has been associated with severe response, including skin atrophy, pruritus, erythema, skin dryness, and suppression of the Hypothalamus-Pituitary-Adrenal gland (HPA) axis ("Drugs.com", 2021). Delivering drug to the intended dermal localised site provides an invaluable specific tool to treat topical conditions permitting the circumvention of skin

barriers, hepatic liver metabolism and systemic side effects (Algahtani *et al*., 2020).

The first-line treatment of PV is composed of local topical agents (Kumar, S. *et al*., 2020). Thus, increase in efficacy of topical therapy should be a priority focus in psoriasis research. Hydrogels have been an interesting field of study since their discovery for biomedical applications. Algahtani *et al* (2020) demonstrated that thermo-responsive hydrogels are used as dual therapy for inflammatory skin diseases - as a drug delivery system and providing moisture to the dry skin(Algahtani *et al*., 2020).

The inflamed area of the psoriasis, after administration of the gel, serves as the peripheral stimulus regulating the activation of the response to release the therapeutic agent, hence in the present study thermo-responsive polymer CMCs will be utilized (López-Saucedo *et al.,* 2019). The hydrogel formulation of corticosteroids such as Mometasone furoate has been shown to be an effective method of delivery of the drug due to high efficacy and low adverse response profile (Kumar, R. *et al*., 2021; Zoabi *et al*., 2021; Kahraman *et al*., 2020).

The purpose of this study was to design a thermo-responsive hydrogel nanoparticle composite system for topical delivery of anti-psoriatic drug (HCT) for the treatment of Psoriasis vulgaris as illustrated in **Figure 1.1**. This hydrogel nanoparticle composite system will have prolonged HCT release into the skin over extended periods.

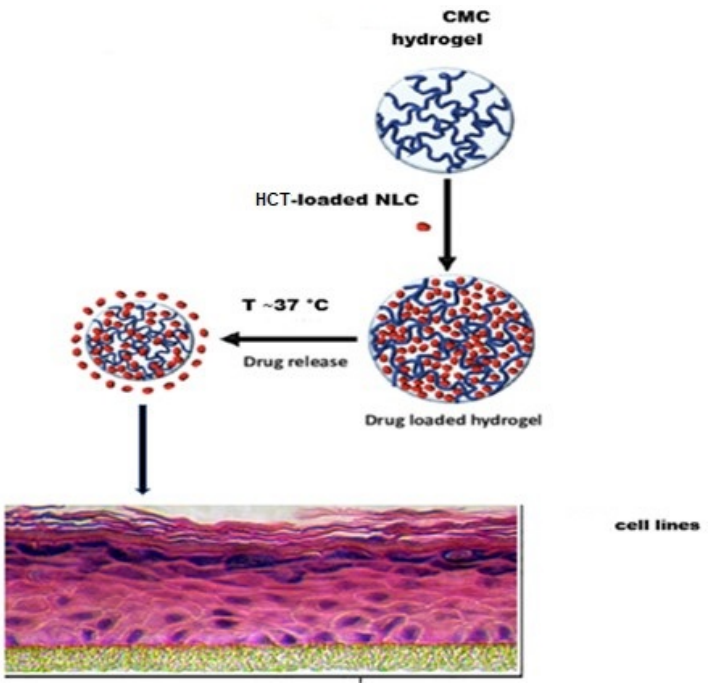


Figure 1.1 Schematic representation of the thermo-responsive CMC hydrogel. The figure illustrates the HCT-loaded SMS-PCL nanoparticle delivery system and its release to the skin cells at approximately 37 ºC (Image from Álvarez-Paino *et a*l., 2017 with modifications).

1.3 Aim and Objectives

The purpose of this study was to synthesise hydrocortisone (HCT) loaded SMS-PCL nanoparticles encapsulated with CMC hydrogel which is responsive to temperature (~37 ºC) for improved transdermal treatment of Psoriasis Vulgaris (PV).

The following objectives were conducted and completed:

1. To synthesize HCT-loaded SMS-PCL nanoparticle delivery system.
2. To evaluate the physicochemical properties of the SMS-PCL nanoparticles, employing Fourier Transformation Infrared Spectroscopy determining molecular state composition of the polymer matrix.
3. To evaluate particle size and surface charge distribution, and determining the uniformity of the SMS-PCL nanoparticles.
4. To evaluate drug entrapment efficacy (DEE) and drug release profiles of the HCT-loaded SMS-PCL nanoparticles and nanoparticles incorporated within the CMC hydrogel employing nanophotometer.
5. To undertake thermal and morphological evaluation, employing Differential Scanning Calorimetry, Thermogravimetric Analysis, and Scanning Electron Microscopy, evaluating the phase transition nature and the particle morphological properties of the HCT-loaded SMS-PCL nanoparticles delivery system, respectively.
6. To evaluate the cytotoxicity of the HCT-loaded SMS-PCL nanoparticles embedded in CMC hydrogel using the MTT (dimethylimidazole diphenyl tetrazolium bromide) assay.

1.4 Overview of this Dissertation

Chapter 1: Serves as the introduction of the dissertation and describes pathophysiology of PV and the challenges faced by individuals suffering from this disease. Current therapies for the PV and the challenges including adverse side effects, lack of patient compliance, lack of availability, and lack of desire for use by patients are also highlighted. Furthermore, this chapter briefly presents hydrogel nanoparticle composite systems as novel drug delivery platforms for the treatment of skin diseases and advantages thereof. Literature from previous studies involving hydrogels is presented as evidence for the efficacy of hydrogels use in the treatment of inflammatory skin diseases. Finally, the aim and objectives of the study are outlined in this chapter.

Chapter 2: is a critical review of transdermal hydrogel drug delivery technologies for the treatment of PV. The drug delivery systems developed for this purpose are elaborated on, in a systematic manner. Recent developments and future goals in transdermal delivery to overcome the

individual limitations of the delivery routes are represented as well. This chapter also reviews the use of hydrogels and their delivery limitations in comparison to that of nanoparticle hydrogel systems, in addition to the various advances in fabrication techniques of gels, providing an update of pharmaceutical research in the field of hydrogel-assisted transdermal drug delivery systems.

Chapter 3: describes the design, materials and methods used, as well as results and discussion for the synthesis of SMS-PCL nanoparticles incorporated within the CMC hydrogel. It explains the characterization of the nanoparticles, conducted utilizing the FTIR, SEM, Zeta sizer, and Thermal analysis. Drug release profiles were determined by dissolution and UV/Vis Spectroscopy. Cell viability studies were also conducted utilizing MTT assay for proof of concept and confirmation of non-toxicity to physiological tissue.

Chapter 4: provides a conclusion and future recommendations in which the study can be enhanced.

CHAPTER 2. A REVIEW OF LITERATURE ON THERMO-RESPONSIVE HYDROGEL SYSTEMS USED IN THE TREATMENT OF INFLAMMATORY SKIN DISEASES

2.1 Introduction

2.1.1 Review of Psoriasis and Current Therapeutic Interventions

Psoriasis is a chronic, incurable, non-communicable, and complex disease with multifactorial courses including genetic predisposition, environmental factors, as well as immunological mechanisms (Rendon and Schakel, 2019). Psoriasis effects primarily manifest in the skin, but may present in other parts of the body such as the scalp, nails, and joints. This disease is classified based on the various dermatological presentations (Rendon and Schakel, 2019; Engler *et al*., 2017): psoriasis vulgaris is the most prevalent form of this disease accounting for 90% of all Psoriasis cases presenting commonly in the trunk and limbs as sharply demarcated, erythematous, pruritic plaque with waxy or silvery scales, inverse (flexural) psoriasis is the type of psoriasis that is localized to areas of the skin that fold (i.e. anogenital area, submammary skin folds, area between fingers/toes, and naval area) and is characterized by scaleless patches and plaques, guttate psoriasis affects children and adolescents; is triggered following streptococcal infection of the tonsils or upper respiratory tract. It presents as small, scaly, erythematous, teardrop-shaped plaques spread across the body. Pustular psoriasis is a form of psoriasis that affects the hands and soles; presents as white pustules, containing sterile, non-infectious pus, and, lastly, erythrodermic psoriasis, which occurs due to an uncontrolled spread of psoriasis covering 90% of the body surface. Erythrodermic psoriasis is potentially life threatening and resistant to treatment.

Psoriasis vulgaris (PV), also known as plaque psoriasis, is the most prevalent form of psoriasis and affects approximately 5% of the world population (Rocha *et al*., 2021). The WHO has declared PV as a severe multifactorial non-communicable disease, with courses attributed to genetic mechanisms, environmental factors, and microbial infections (Afonina *et al.,* 2021; Iskandar *et al*., 2021). Clinically, PV presents with scaly itching, oedema, fatigue, burning, and erythema, as seen in **Figure 2.1**.

The severity of PV is determined by the surface area affected. When less than 3% of the body surface area is affected, this is classified as mild PV. Moderate PV is classified when 3% to 10% of the body surface is affected. Lastly, when more than 10% of the body surface is affected, this is classified as severe PV (Engler *et al.*, 2017). In addition to its negative effects on the skin, PV is further associated with numerous secondary illnesses, such as obesity, hypertension, vascular inflammation, psoriatic arthritis, metabolic syndrome, irritable bowel syndrome (IBS), and may have psychiatric manifestations (Pannu and Rosmarin, 2021; Yang and Kourosh, 2018). Furthermore, this disease can affect the lifestyle of the patients, leading to the use/misuse of nicotine and alcohol (Sterry *et al.*, 2014) (**Figure 2.2**). One of the hallmarks of the PV disease is hyperproliferation of keratinocytes (hyperkeratosis), which triggers an immune response by activating immune cells and releasing cytokines (Limón *et al.*, 2019;Boehncke and Schön, 2015).

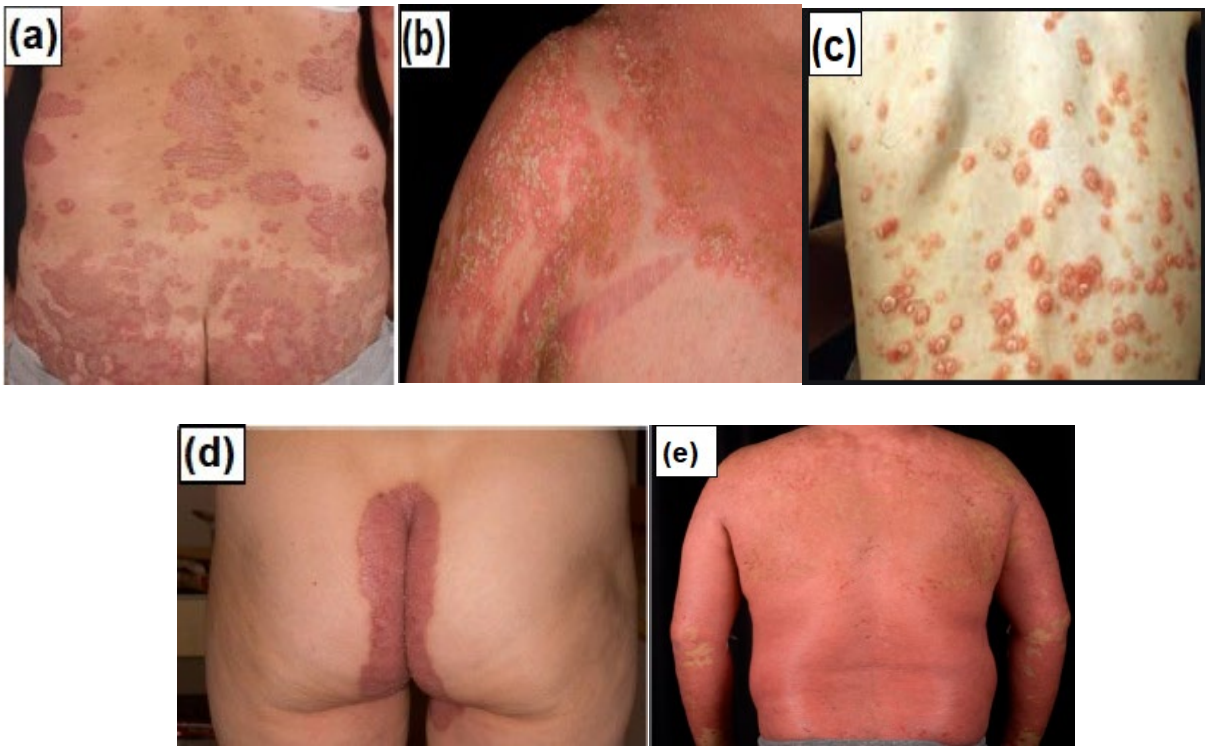


Figure 2.1 Clinical Presentation of Psoriasis. The above figure shows different classifications of psoriasis. Figure 2.1(a) shows Psoriasis vulgaris, (b) Pustular psoriasis, (c) Guttate psoriasis, (d) Inverse psoriasis, and (e) Erythrodermic psoriasis. (Images used with permission from Rendon and Schakel, 2019).

When triggered by various factors, such as environment, stress, trauma, and pathogens, dendritic cells release cytokines that lead to a sustained psoriatic inflammation (Rendon and Schakel, 2019). Interleukin 23 (IL-23) and Tumour Necrosis Factor (TNF)α are released by the innate immune system upon trigger by the various factors stated above. These, in turn, are involved in the proliferation, differentiation, and effector function of helper T cells 17 (Th17) lymphocytes (Baliwag *et al.,* 2015). Current developments in inflammatory disease research show that the IL-23-TNFα-Th17 axis plays a major role in psoriasis vulgaris (Schön and Erpenbeck, 2018). Th17 cells play an important role in the pathogenesis of psoriasis through the release of IL-17A, IL-17F, IL-22, and TNFα which have been found in psoriatic lesions; and are responsible for the hyperproliferation of keratinocytes (a hallmark of the psoriasis disease). Treatment interventions aimed at inhibition of the IL-23-TNFα-Th17 axis using Methotrexate (MTX) have demonstrated significant decrease in serum levels of IL-17 – leading to improved state of the psoriasis in individuals suffering from this disease (Budamakuntla *et al*..2017).

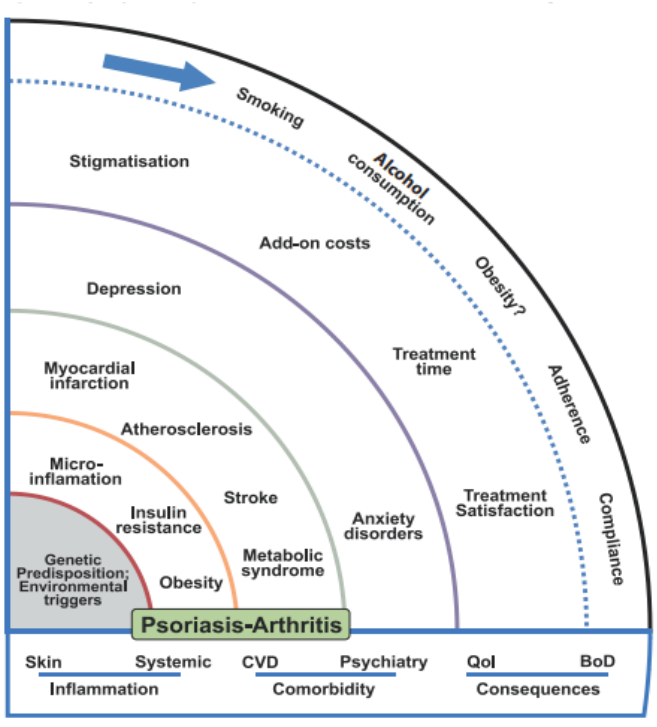


Figure 2.2 Effects of Psoriasis. In this figure, the effects of psoriasis are shown from the skin, systemic effects, secondary diseases (cardiovascular disease (CVD) and psychiatric reactions), to the effects on the overall quality of life (Qol) and burden of disease (open source image obtained from WHO, 2016).

PV is an incurable disease. As such, therapeutic strategies are aimed at managing the symptoms of this disease and improving the quality of the patients' lives. The treatment of PV depends on the severity of the disease (Al Raddadi *et al.*, 2011). Three treatment options exist: topical therapies, phototherapy, and systemic therapies which can be prescribed alone, or in combination subject to disease progression and severity (Jacobs and Kgokolo, 2020; Steinhoff *et al*., 2020; Meng *et al.*, 2019).

South African treatment guidelines recommend for the use of corticosteroids as a standard of care for this disease (Jacobs and Kgokolo, 2020; Steinhoff *et al*., 2020). Topical corticosteroids are prescribed as a first-line therapy for PV for localised and mild forms of this disease (Chiang and Verbov, 2014). The severe form of this disease is treated with systemic therapy using MTX, Acitetrin, and Cyclosporin A. Additionally, biological mechanism can be utilised. These include, IL-23 antagonists, T-cell targeted therapeutics, as well as TNFα inhibitors (Abdulghani *et al*., 2011). Hydrocortisone, methylprednisolone acetonate, mometasone furoate, betamethasone valerate, and dexamethasone are some of corticosteroids utilized (Lyseng-Williamson, 2016). These show efficacy as therapeutic agents against PV; however, they are associated with undesirable local and systemic side effect, such as skin atrophy, pruritus, erythema, skin dryness, and suppression of the Hypothalamus-Pituitary-Adrenal gland (HPA) axis ("Drugs.com", 2021).

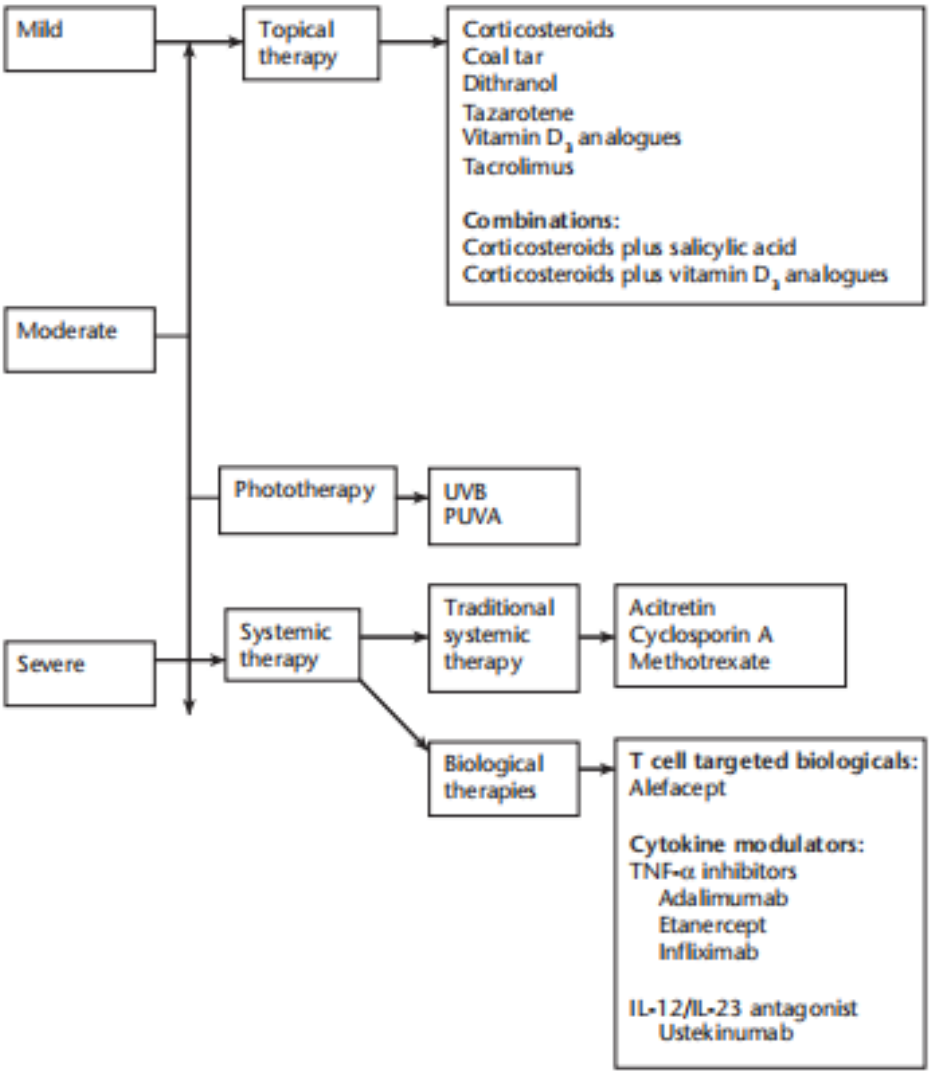


Figure 2.3 Treatment of mild, moderate, and severe psoriasis. *UVB = ultraviolet B-rays; PUVA = psoralen and ultraviolet A (Image adapted from Raboobee *et al.*, 2010).

Other factors contributing to the limited utilization of topical corticosteroids are: lack of compliance by patients, needs for frequent application of the medication, cost and availability of the medication, and lack of adequate knowledge about the disease (Wang *et al.*, 2016; Chatterjee *et al.*, 2018). In a review by Belinchón *et al*. (2016), patient satisfaction, compliance, and preference for psoriasis therapy was investigated. **Table 2-1** summarizes data obtained looking at aspects of patient adherence, patient satisfaction with therapy, and patient-preferred therapy. In the review, data under each category is given for the four therapy types (topical [creams, lotions, ointments], phototherapy [UV], systemic [oral tablets, injections], and biological agents [TNFα inhibitors]).

Table 2-1 Treatment Adherence, Satisfaction, and Preference in Psoriasis.

Therapy type		Percentage (%)	Instrument Used	References
Patient Adherence to duration of therapy	Topical Phototherapy Systemic therapy Biological agents	71 80 82 95*	Patient self-reported measures	Belinchón et al. (2016); Hsu. and Gniadecki (2016)
Patient Satisfaction	Topical Phototherapy Systemic therapy Biological agents	18 10 38 44	Treatment Satisfaction Questionnaire for Medication (TSQM)	Belinchón *et al*. (2016)
Patient Preference	Topical Phototherapy Systemic therapy - Oral - Injected Biological agents	34 14 28 17 38	TSQM	Belinchón *et al*. (2016)

Based on the above table, it is evident that patient satisfaction with conventional therapy is significantly low; which in turn affects adherence. Thus, this demonstrates the need for new novel and efficacious therapeutic interventions.

2.2 Topical Drug Delivery

The skin can be described as the largest, continuous organ the human body has (Wong *et al.*, 2016). The skin functions as a mechanical barricade for external defence against pathogens and environmental toxins, furthermore, it aids in maintaining a constant internal environment (homeostasis) (Marieb and Hoehn, 2012).

2.2.1 Anatomy of the skin

Anatomically, the skin is comprised of two (2) distinct regions, the outer epidermis and the inner dermis. **Figure 2.4** illustrates the normal anatomy of the skin. The epidermal layer is the outermost skin layer of the skin made up of four layers (in order): (i) stratum basale, (ii) stratum spinosum, (iii) stratum granulosum, and finally (iv) stratum corneum (OpenStax College, 2015). A key challenge in topical delivery of therapeutic compounds is the inability of therapeutic compounds to penetrate the stratum corneum (Salgado *et al.*, 2014;Ruela *et al.*, 2016). The stratum corneum permits passage of molecules that are below 500 Da in size (Rapalli *et al.*, 2020). As a result of this, most corticosteroid formulations, such as ointments, lotions and creams, prove to be ineffective as therapeutic agents and uncomfortable for patients due to the need for frequent application (Lyseng-Williamson, 2016; Panonnummal *et al.*, 2017). Some of the corticosteroids used in the treatment of psoriasis, such as Hydrocortisone, Dexamethasone, and Mometasone furoate have molecular sizes of 362 Da, 392 Da, and 427 Da, respectively ("Royal Society of Chemistry", 2020). Another critical factor for drug permeation across the skin is the partition coefficient (*LogP*) – which is a commonly used method of measuring lipophobicity. Compounds possessing a larger *LogP* are more effective and faster preheaters of the stratum corneum – which in turn makes them more efficacious for topical drug delivery (Kang *et al*., 2007).This permits intercellular penetration of these compounds across the stratum corneum. Additionally, the altered architecture of the skin in psoriasis presents a greater challenge due to hyperplasia of the epidermis (hyperkeratosis) which significantly reduces the permeation of therapeutic compounds (Ghate *et al.*, 2019). To ensure effective topical delivery of therapeutic agents, newer formulations with capacity to permeate the stratum corneum and be maintained in the skin for a prolonged amount of time need to be developed.

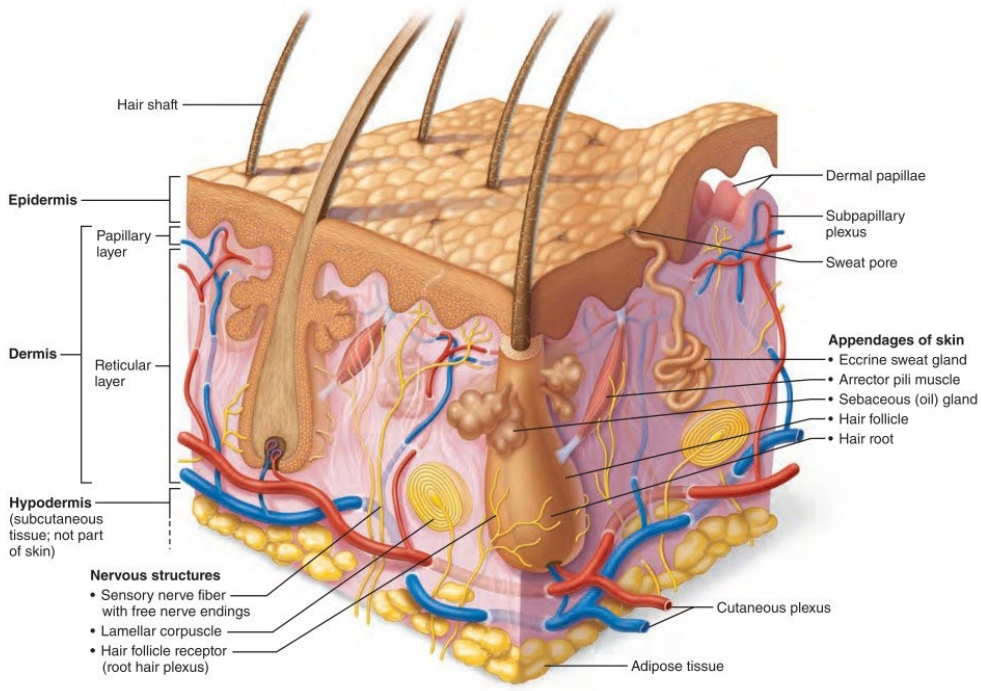


Figure 2.4 Anatomy of the Skin. The 3D figure shows the distinct skin layers. The outer epidermis is a keratinized superficial layer of the skin, deep to that is the dermis, a highly vascularized layer (Image obtained from Marieb and Hoen, 2012).

2.2.2 Drug Delivery across the skin

Delivery of drugs topically is the keystone of drug delivery in the management of inflammatory skin diseases (Al Raddadi *et al.*, 2011). This method of drug delivery is appealing as it circumvents the drawback associated with the oral route of administration (Alexander *et al.*,2012). Drugs administered through this route exhibit a local effect where it is desired (Wang *et al.*, 2019;Whalen *et al.*, 2017). Advantages of this route of administration include: avoidance of the harsh gastro-intestinal environment, avoidance of first-pass metabolism by the liver, drug release is prolonged and sustained, application of therapy is easy and convenient, minimal occurrence of systemic side effects, acceptance and compliance by patients, bioavailability is improved, and drug delivery is selective and localized (Nikolić *et al.*, 2019;Sharadha *et al.*, 2020).

The therapeutic potential of current conventional therapies is limited by a number of drawbacks: lack of patient satisfaction and compliance with the therapy (Haidari *et al.*, 2020), lack of availability and cost of therapy, and side effect profiles of the therapy (Strober *et al.*, 2019). When

considering PV, the first-line treatment is composed of local topical agents (Al Raddadi *et al.*, 2011). Thus, increase in efficacy of topical therapy should be a priority focus in psoriasis research. Hydrogels have demonstrated great potential as therapeutic agents against PV (Wang *et al.*, 2016).

2.2.3 Hydrogels as potential therapeutic agents

Since their discovery, hydrogels have been an interesting topic to scientists for biomedical applications (Silna *et al.*, 2016). Unlike conventional therapies, hydrogels surmount the skin barrier, allowing them to deliver drugs to their site of action while ensuring sustained drug release, high retention of drug, high bioavailability, ease of application, optimal drug concentration, minimal risk of adverse events occurrence, and cost effectiveness (Rapalli *et al.*, 2020). Furthermore, hydrogels are more acceptable to patients, thus show potential to eliminate barriers in PV therapy and improve clinical outcome (Lyseng-Williamson, 2016).

This review aims to provides an in-depth view of a class of hydrogels known as thermo-responsive hydrogels. These are hydrogels that respond to temperature as a stimulus and their potential application in the treatment of PV. The review will further look into the physicochemical characteristics and properties of the natural and synthetic polymers that enable their thermo-responsive behaviour. Hydrocortisone, Dexamethasone, and Mometasone furoate (MF) used in the management of corticosteroid-responsive dermatoses (skin diseases) possesses great potential as novel therapeutic outlets for the treatment of PV. The basis for the use of the above polymers and drugs as constituents for the topical thermo-responsive hydrogel drug delivery platform for the treatment of PV will be discussed in detail in the sections to follow.

2.3 Hydrogels

By definition, hydrogels are three-dimensional (3D), porous, hydrophilic, cross-linked polymeric networks with the ability to retain large amounts of biological fluids or water, and swell without losing their structure (Chatterjee *et al.*, 2018; Wang *et al.*, 2016; Kumarasamy *et al.*, 2018). Hydrogels have gained a considerable amount of interest for numerous biomedical applications, including, but not limited to, tissue engineering, wound dressing, contact lenses manufacturing, hygiene products, and, of particular interest, drug delivery (Caló and Khutoryanskiy, 2015). Hydrogels are diverse; they can be made up of natural or synthetic polymers, chemically or physically cross-linked, and biodegradable or non-biodegradable (Hoffman, 2013). Some hydrogels are referred to as "smart hydrogels" due to their ability to respond to external chemical or physical stimuli: pH, electric current, ionic strength, metabolites, light, and temperature (Li *et al.*, 2021; Huang *et al.*, 2019; Chen *et al.*, 2020). The most commonly studied class of hydrogels are thermo-responsive hydrogels as possible drug delivery platforms for multiple therapeutic indications because temperature is considered an important physiological parameter. Due to their nature, they have become a viable candidate for topical drug delivery in inflammatory skin diseases, such as atopic dermatitis and psoriasis vulgaris (Wang *et al.*, 2016; Limón *et al.*, 2019).

2.3.1 Thermo-responsive Hydrogels

Thermo-responsive hydrogels are capable of altering their structure in response to changes in temperature (Thakur *et al.*, 2018). They remain in a liquid phase at low temperatures (e.g. room temperature of ~20-25 ºC) and transform into gels when their critical solution temperature (CST) is reached. CST is the temperature at which the solution reaches miscibility completely, thus exhibiting a sol-gel transition phase. Hydrogels with lower critical solution temperature (LCST) reach this phase when the temperature is raised **(Figure 2.5. (a))**. Conversely, hydrogels with upper critical solution temperature (UCST) reach the sol-gel transition phase when temperature is lowered (**Figure 2.5 (b)**) (Don *et al.*, 2008).

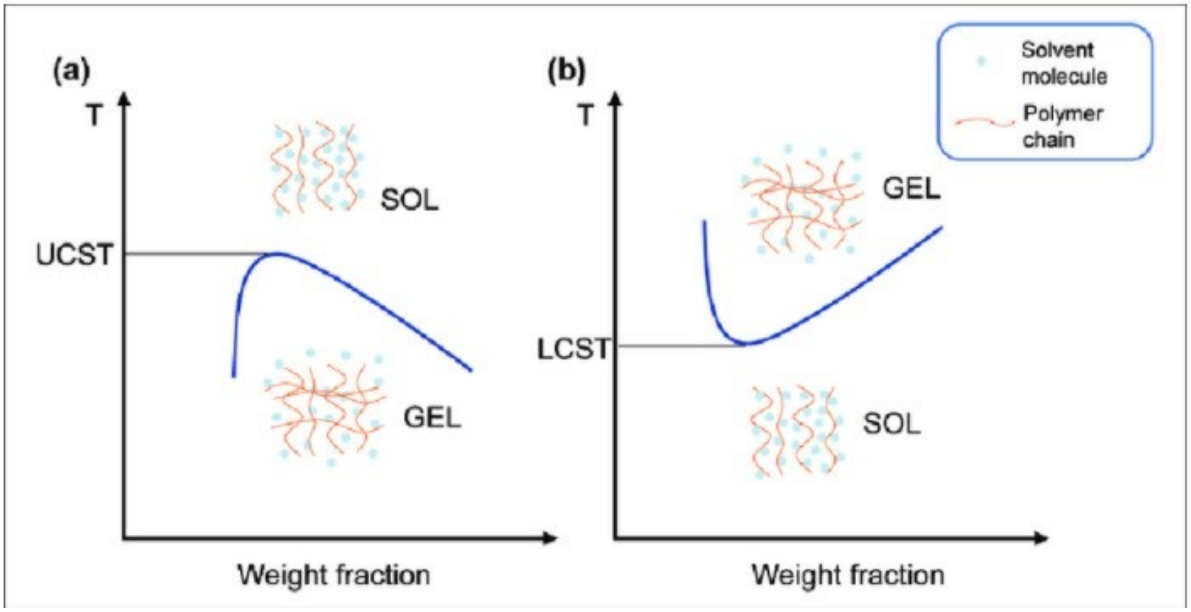


Figure 2.5 Illustration of UCST and LCST in thermo-responsive hydrogels. The figure shows the sol-gel transition of hydrogels when a specific temperature (CST) is reached (adapted from Altomare et al., 2018).

In the case of biomedical application, the hydrogels exhibiting LCST are of particular significance since they are able to instantly form gels when physiological temperature of ±37 ºC is reached (Klouda, 2015). Hydrogels with LCST contract when the temperature is increased (from ambient temperature to physiological temperature), allowing for release of drug molecules under these conditions (Li *et al.*, 2021).

The common release mechanism of drug molecules from the hydrogel (once LCST is reached) is passive diffusion (Huang *et al.*, 2019).

The inflamed area of the skin in PV, following administration of the gel, serves as the peripheral stimulus for the release of the therapeutic compound. **Table 2-2** summarises some of the widely studied thermo-responsive polymers, for both natural and synthetic polymers and their respective CST:

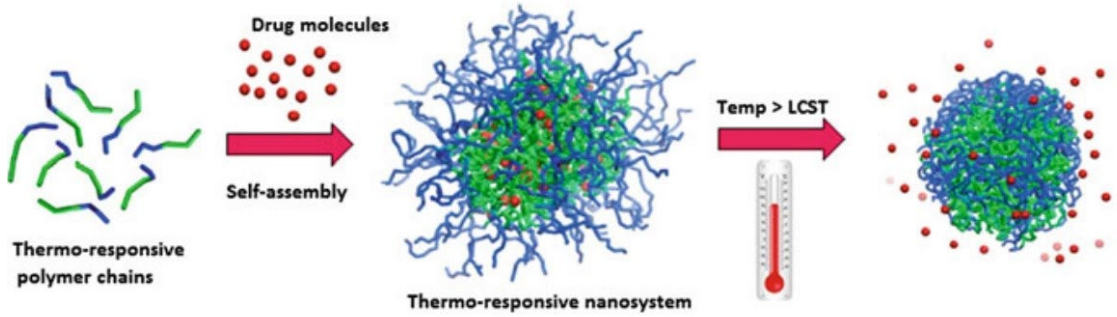


Figure 2.6 Schematic representation of the thermo-responsive hydrogel system. This figure shows the process of drug release when LCST of the hydrogel is reached. (Image used with permission from Lale and Koul, 2018).

Table 2-2 Summary of widely studied polymers. The CST is provided for each respective polymer.

Polymer		PTT* (ºC)	Reference(s)
Synthetic Polymers	poly-N-Isopropylacrylamide (pNIPAAm)	32	(Li *et al.*, 2021 Don *et al.*, 2008; Thakur *et al.,* 2018)
	Polyethylene Glycol (PEG)	120	(Huang *et al.*, 2019)
	Polypropylene Glycol (PPG)	50	(Huang *et al.*, 2019)
	POx family:		
	- poly(2-methyl-2-oxazoline) (PMOx)	None	
	- poly(2-ethyl-2-oxazoline) (PEOx)	60	
	- poly(2-isopropyl-2-oxazoline (PiPOx)	36	(Kim and Matsunaga, 2017)
Natural Polymers	Cellulose		
	- Carboxymethyl cellulose (CMC)	60	
	- Hydroxypropyl cellulose (HPC)	45	(Klouda, 2015; Chatterjee, Hui and Kan, 2018)
	- Hydroxypropylmethyl cellulose (HPMC)	69	(Klouda, 2015)
	Gelatin	<25	
	Agarose	34	(Graham *et al*., 2019)

**PTT= Phase-Transition Temperature*

2.3.1.1 Natural polymers

A prerequisite for the successful utilization of hydrogels as polymeric drug delivery platforms is biodegradability, biocompatibility, and high degree of stability; this is the cornerstone of polymeric drug delivery research (Kim and Matsunaga, 2017). This makes natural polymers more advantageous to use as they are more cheap, none-toxic, biocompatible, and biodegradable when compared to their synthetic counterparts (Gyles *et al.*, 2017).

Cellulose

Cellulose is the most abundant polymer occurring in nature, and is found as the main component of plant cell walls (Rimmer, 2011). Naturally occurring cellulose is hydrophobic; however, cellulose derivatives are hydrophilic, allowing for their use as hydrogel components. Cellulose derivatives have been extensively investigated for their use as vehicles in drug delivery research due to their biocompatibility and biodegradability, and their "smart" polymer behaviour with the ability to respond to temperature as a stimulus (Ciolacu *et al.*, 2020). Wang *et al.* (2016) demonstrated the effective utilization of carboxymethyl cellulose (CMC), an extensively studied cellulose derivative, in combination with Poloxamer407 (P407) as a possible drug delivery platform in Atopic dermatitis. CMC can also be used as a co-polymer in hydrogels to aid in the design of a suitable hydrogel structure. In a study conducted by Nita *et al.*, (2020), co-polymerization of poly(2-Dimethylaminoethyl methacrylate) with CMC, confirmed its use as a potential drug delivery system for transdermal patches by lowering the LCST from 42 ºC-47 ºC to 37 ºC. Further investigations of this polymer need to be carried out for its potential use in psoriasis vulgaris.

Gelatin

Gelatin is a polymer resulting from partial hydrolysis of collagen (either by acid or base) wich excellent degree of biocompatibility and biodegradability; making it highly utilizable in hydrogel systems (Rodríguez-Rodríguez *et al*., 2020; Thakur *et al*., 2018). The conformation of gelatin changes when temperature is decrease below 35 °C (UCST), and solidifies below room temperature (<25 °C) (Huang, 2019; Chatterjee *et al*., 2018). As this is not ideal in the physiological setting, which requires polymers to gelate at temperatures above 35 °C, gelatine has been co-polymerized with other polymers – such as chitosan and poly(N-isopropyl acrylamide)

(pNIPAAm) - to enable it to exhibit thermo-responsive properties at temperatures closer to body temperature of 37 °C (Chatterjee *et al*., 2018). Cheng *et al*. (2019), successfully synthesised a gelatine/chitosan hydrogel delivery system for ophthalmic drug delivery with a sol-gel transition temperature of 35 °C. Thus proving that gelatine -when copolymerized with other polymers- is an ideal candidate as a thermo-responsive nanopolymeric drug delivery system.

Agarose

Agarose is a naturally-occurring, linear polysaccharide derived from algae used widely in biomedical applications (including as a gel for electrophoresis). Agarose ha a melting point of 80-90 °C and reaches point of gelation when cooled down (UCST) to approximately 34 °C (Yazdi *et al.*, 2020; Graham *et al*., 2019). It has been demonstrated that agarose hydrogels are well suited for application in wound dressings due to their biocompatibility (Graham *et al*., 2019). To lower the gelation temperature, agarose can be synthetically methylated. The degree of methylation of agarose has an impact on the gelation temperature (UCST). This ability can be exploited to utilize agarose as a potential thermo-responsive hydrogel system for topical drug delivery in PV.

2.3.1.2 Synthetic polymers

Unlike natural polymers, synthetic polymers are more stable in terms of physical, chemical, and mechanical properties, however, they are expensive to manufacture (Croisfelt *et al*., 2019). Synthetic polymers have also been extensively studied as novel outlets for drug delivery. Some of the most widely studied synthetic polymers are poly(N-isopropyl acryl amide) (pNIAAm), polyethylene glycol (PEG), and polycaprolactone (PCL).

pNIAAm

PNIAAm is an extensively studied synthetic polymer that exhibits thermo-responsive behaviour with a LCST of approximately 32 °C; above this temperature, an opaque gel forms as the polymeric solution transforms (Croiselt *et al*., 2019). Numerous applications of pNIAAm has been

studied, including use in wound healing, tissue engineering, stem cell transplantation, cancer cell imaging, and drug delivery (Lanzalaco and Armelin, 2017). To ensure the applicability of pNIAAm as a drug delivery platform, the degree biocompatibility and biodegradability of this polymer has to be increase. This can be achieved through copolymerization or crosslinking with other natural polymers, polyssacharides, or proteins (Tipa *et al*., 2021). Furthermore, copolymerization of pNIAAm with hydrophylic monomers results in an increased LCST that is closer to physiological temperature of 37 °C; making it suitable for biomedical application (Chatterjee *et al*., 2018).

2.4 Corticosteroids

Mometasone furoate (MF) [MW = 521.4 g/mol; chemical formula = $C_{27}H_{30}Cl_2O_6$, LogP = 4.115] is a class III potent corticosteroid derivative of hydrocortisone prescribed for the treatment of allergic rhinitis, asthma, and inflammatory skin conditions (SAMF, 2016). MF possesses anti-pruritic, vasoconstrictive, and anti-inflammatory properties. MF 0.1% formulation is effective and well tolerated, thus it has been approved for the treatment of psoriasis diseases (Greive and Barnes, 2016).

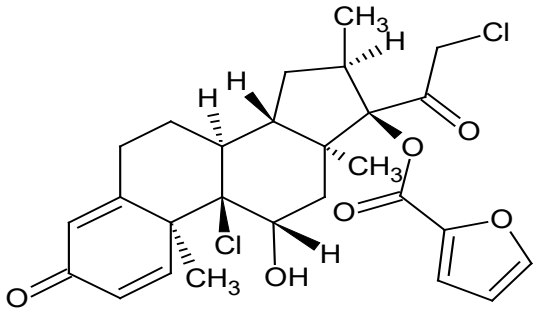


Figure 2.7 Structure of Mometasone furoate (MF).

Hydrocortisone (HCT) [MW = 362.5 g/mol, chemical formular = $C_{21}H_{30}O_5$, Log*P* = 1.61] is a class V-VII, low-to-intermediate-potency corticosteroid (analogous to the hormone produced by the adrenal glands) with anti-pruritic, anti-inflammatory, and vasoconstrictive effects. The hormone possesses primary glucocorticoid and minor mineralocorticoid effects. HCT promotes suppression of the immune and inflammatory responses ("PubChem", 2020). HCT is indicated for use (topically) in the treatment of eczema, pruritus, dermatitis, and psoriasis (SAMF, 2016)

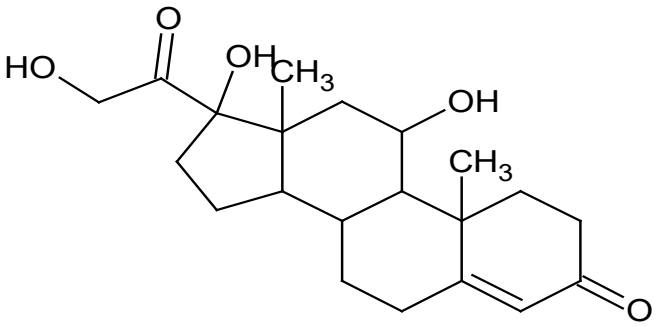


Figure 2.8 Structure of Hydrocortisone.

Dexamethasone (DEX) [MW = 392.5 g/mol, chemical formular = $C_{22}H_{29}FO_5$, LogP = 1.83] low-potency class VII corticosteroid indicated for use in treatment of various dermatoses, endocrine, rheumatic, allergic, ophthalmic, gastrointestinal, respiratory, haematologic, neoplastic, and oedematous confitions (”Drugbank”, 2021).

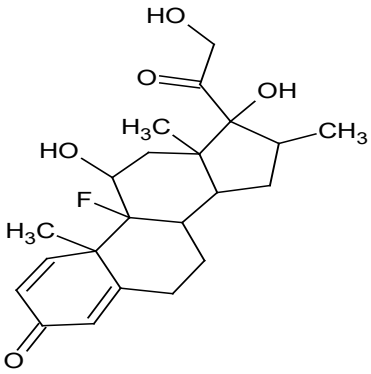


Figure 2.9 Structure of Dexamethasone.

Corticosteroids can be found in a variety of formulations to enable their use in different clinical indications, examples of these are listed below:

Table 2-3 Various Corticosteroid Formulations and Their Respective Trade Names.

MF	HCT	DEX
▪ Cream - *Elocon®* ▪ Ointment - *Momexin* ▪ Lotion – *Elocon®, Zetamil*	▪ Lotion – *Ala-Scalp* ▪ Cream – Alacort ▪ Suspension - *Colocort* ▪ Ointment -	▪ Tablet - *Decadron* ▪ Elixir - *Baycadron* ▪ Liquid (Injection) - *Dexicu*

▪ Inhalant – *Asmanex Twisthaler, Asamex HFA* ▪ Nasal spray - *Nasonex®, Sinuva* ▪ Hydrogel – *Zatamil (Australia)*	▪ Tablet - *Cortef*	▪ Suspension – *Maxidex, Ciprodex* ▪ Ointment – *AK-Trol* ▪ Implant - *Ozurdex*

2.4.1 Pharmacokinetics

2.4.1.1 Absorption

Topical formulations of corticosteroids are absorbed through the skin. Owing to its high lipophilicity, MF is able to penetrate the stratum corneum of the skin (**Figure 2.4**) to reach the viable epidermis at high therapeutic concentration – approximately 94% retention (Salgado *et al.*, 2014; Spada *et al.*, 2018). In contrast, upon absorption, HCT has been observed to only have a bioavailability of up to 19%, and 78% for dexamethasone (oral), respectively ("Drugbank", 2020). The degree of stratum corneum penetration is significantly affected by the topical delivery vehicle (formulation) of the corticosteroid as well as the degree of integrity of the skin. Hydrogels demonstrate better permeation with less binding to stratum corneum components, making them idea drug delivery platforms in PV.

Distribution

Topical corticosteroids are associated with low systemic distribution due to local effect exhibited by this class of drugs. The systemic bioavailability of MF 0.1% has been reported to be 0.7% over an 8-hour period after dosing in non-occluded skin (Merck, 2013; Spada *et al.*, 2018).

Metabolism

HCT, DEX, and MF 0.1% are metabolized by the hepatic enzyme, Cytochrome P450 3A4 to yield 6-β hydrocortisol, 6-α and 6-β hydroxydexamethasone, as well as free mometasone and 6-β-hydroxymometasone as primary metabolites, respectively ("Drugbank", 2021; Wohlrab *et al.*, 2016)

Excretion

Because very minimal systemic absorption of MF 0.1% occurs, there is no observation of plasma metabolites of MF. Elimination of MF and its metabolites is through urine, where only 0.00076% of the originally administered dose is found (Spada et al., 2018). The elimination half-life of MF is 5.8 hours.

2.4.2 Pharmacodynamics

Mechanism of Action

Corticosteroids bind selectively, to corticosteroid receptors in the epidermis. MF binds with greater affinity as compared to other corticosteroid of similar or weaker potency – 22-times greater affinity compared to dexamethasone, 2 to 4-fold greater affinity than hydrocortisone. Binding of MF to receptor promotes expression of anti-inflammatory protein (phospholipase A_2), which in turn acts by inhibition of the arachidonic acid pathway (Merck, 2013; Spada *et al.*, 2018).

2.5 Treatment of Psoriasis: Recent Topical Applications

As discussed earlier, PV is a chronic incurable inflammatory disease, thus aim of PV therapy is to alleviate the symptoms for the individuals affected by this disease. Topical treatment is the keystone of PV therapy (Armstrong and Read, 2020; Al Raddadi *et al.*, 2011). Currently, the severity and burden of PV is measured and assessed through the Psoriasis Area and Severity Index (PASI) and body surface area (BSA). The PASI score (used to calculate the percentage of PV clearance [e.g. PASI-75 means 75% reduction in PV]) and low BSA (<10%) are good indicators of disease improvement in PV therapy (Svoboda *et al*., 2020). Additionally, patient-reported measures take into account other critical aspects of PV, such as quality of life (QoL). These are taken into account to better understand and close the gap between physicians' treatment goals and patient-preferred outcomes (Svoboda *et al*., 2020; Suresh *et al*., 2013). In this section, recent topical treatment strategies – in terms of creams, foams, nanoparticles, and hydrogels - for PV are explored.

2.5.1 Topical Creams

Topical corticosteroid creams are prescribed as first line therapy for the management of PV (Vincent *et al.*, 2014). The class of corticosteroid cream prescribes differs based on the severity of the disease. Class I (high potency) corticosteroids are prescribed for sever forms of PV, while class VII (low potency) corticosteroids are prescribed for mild forms of this disease (Armstrong and Read, 2020; Kleyn *et al*., 2019).

Betamethasone dipropionate 0.05% (BM) cream is a potent topical corticosteroid used in the management of psoriasis. However, prolonged use of BM is associated with adverse skin reactions. Tazarotene (TAZ) is an excellent retinoid shown to have high efficacy against PV. Chen *et al*. (2020) studied the effects of a fixed dose combination of BM/TAZ, TAZ alone, and BM alone, respectively, over a period of 6 weeks in 600 Chinese patients with PV. The study found that 44% of participants in the BM/TAZ combination achieved over 75% reduction (PASI-75) of psoriatic lesions, with this number being lower for the TAZ alone and BM alone arms (19% and 35%, respectively). Furthermore, a recurrence of PV was 10,6% for BM/TAZ, 10% for TAZ, and as high as 30% for BM after withdrawal of the therapeutic for 2 months. Thus concluding that the BM/TAZ is effective against PV, has minimal adverse side effects profile, and with low relapse/recurrence rates of PV compared to the corticosteroid, BM.

In another study, MF 0.1% was utilized as a model corticosteroid in a cream composed of linoleic acid (LA)-Ceramides (Cer) [LA-Cer-MF]. The aim of this study was to counteract the harmful effects of corticosteroids that lead to breakdown of stratum corneum lipid composition (Li *et al*., 2020). Following a 12-week treatment period, the PASI score was >50% in participants receiving the LA-Cer-MF treatment. However, the study recorded side effects ranging from exacerbation of PV, skin dryness, subcutaneous haemorrhage, skin atrophy, peripheral folliculitis, and erythema. Overall, the study demonstrated that the LA-Cer cream aids in prolonging the improvement effects of corticosteroids and aids in alleviating symptoms of PV (Li *et al*., 2020)

Topical creams are a first-line effective therapy for the treatment of PV. However, they are accompanied by many limitations and barriers to efficacy (Armstrong and Read, 2020). They are associated with undesirable adverse local effects (skin irritation, skin atrophy, telangiectasia, erythema, pruritus, skin dryness) (Chen *et al*., 2020; Segaert *et al*., 2020; Kleyn *et al*., 2019), as well as systemic effects (HPA suppression, adrenal insufficiency) (Alahmadi *et al*., 2020). In addition to the drug effects, patient compliance is a major issue is PV therapy. Factors contributing

to this include high rate of reported adverse side effects (~35%), dissatisfaction with medicine requirements, and impact of PV therapy on QoL (Svoboda *et al*., 2020; Segaert *et al*., 2020; Kleyn *et al*., 2019). In light of this, a need for novel efficacious therapeutic interventions in evident.

2.5.2 Topical Aerosol Foams

Foams are currently used clinically for as innovative, long-term PV therapy. This formulation is advantageous as it allows long-term adherence and higher convenience for management of chronic skin diseases (Wollina *et al.*, 2019; Richards *et al*., 2006). When compared to lotions and creams of the same class, foams have demonstrated n increased efficacy in treatment of psoriasis of the scalp (Yang and Lipner, 2021).

A fixed combination of calipotriol and betametasone dipropionate (Cal/BD) foam (Enstilar®) is a Vitamin D3 analogue and corticosteroid combination foam administered once daily for adults with mild to moderate PV (Huang *et al*., 2019). Cal/BD is currently on the market and has demonstrated better tolerability and efficacy than betamethasone cream/ointment. Clinical trial data demonstrated that this anti-psoriatic foam formulation is more effective and well tolerable more than systemic therapies (Kim and Frampton, 2016). Clinical trial data has shown more than 90% (PASI-90) clearance of plaque after once-daily Cal/BD treatment over a period of 1 month (Dattola *et al*., 2020).

In another clinical trial, Gold et al., (2016) sought to compare the efficacy of the foam formulation against ointment. They also proved that Cal/BD aerosol foam was significantly more effective than Cal/BD ointment and the individual active ingredients for treating PV, resulting in greater and faster reduction in disease severity and rapid, effective relief of itch.

Combination of topical tazarotene and betamethasone valerate foam provides enhanced efficacy and a better side-effect profile compared with either agent when used alone. In this study, 10 patients with localized PV were treated with betamethasone valerate foam (0.12%) in the morning and topical tazarotene cream (0.1%) in the evening for a total of 12 weeks or until plaques cleared, whichever occurred first. Individual plaque characteristics (erythema, scale, and thickness) and a PASI score were determined at weeks 4, 8, and 12 of the study. The study reported that 89% of patients experienced improvement of their disease by week 12. Two patients (20%) were clear of their psoriasis at week 4, and the other 4 patients were clear at week 8 with 0% adverse events reported. The combination of tazarotene cream and betamethasone valerate foam is an effective

combination approach to treating localized PV. There was no irritation reported, implying that the use of corticosteroid foam may protect against the potential local irritation reported with tazarotene (Dhawan *et al*., 2005).

2.5.3 Hydrogels for Topical Applications

Mao *et al*., (2017) designed skin-permeating nanoparticles that enable delivery of curcumin (a TNF-α inhibitor) to the deeper layers of the skin. A silk fibroin (SF) hydrogel was designed; in which curcumin nanoparticles were loaded. The study reported that the SF hydrogel enhanced the skin permeation capability of curcumin. In turn, this was responsible for an improved response in PV model (Saleem *et al*., 2020).

Curcumin – an herbal substance with anti-inflammatory properties – was further studied in mouse models for antipsoriatic effects. Morankar *et al*. (2021) aimed to increase the permeability and solubility of this compound through incorporation into a hydrogel formulation. This showed a 9.17% decrease in inflammation on the tails of the male Wistar rats used in the experiment (Morankar *et al*., 2021).

Methotrexate (MTX) is widely used in cancer and autoimmune diseases (such as inflammatory skin diseases). To circumvent adverse events associated with systemic administration of MTX, hydrogels can be utilized as a viable topical delivery vehicle (Dehshahri *et al*., 2021). MTX was encapsulated in liposomes and loaded in hydrogels and studied in patients with localized PV (Ali *et al*., 2008). This study reported that once daily of the MTX-loaded hydrogel improved adherence to treatment, produced minimal adverse reactions, and demonstrated a sustained release of MTX compared to MTX alone (Ali *et al*., 2008).

Kaur et al. (2018) successfully synthesised a Nanostructured Lipid Carrier-based hydrogel loaded with MF for the treatment of psoriasis. *In vivo* studies demonstrated complete clearance of parakeratosis in Wistar rat models. Additionally, the hydrogel formulation provided 2.5 times higher skin deposition of the drug, as well as prolonged drug release, in comparison to the conventional cream formulation. Thus confirming this hydrogel formulation as a potential drug delivery vehicle of the antipsoriatic drug, MF, in the treatment of PV.

Literature based on hydrogels shows these as promising drug delivery systems for the management of inflammatory skin diseased such a PV due to their enhanced permeability and sustained drug release.

2.6 Concluding Remarks

Thermo-responsive polymeric hydrogel systems have been extensively studied for possible application as topical drug delivery platforms. Based on the literature, CMC is a highly thermo-reversible compounds, with potential for therapeutic application in inflammatory skin diseases as a polymeric hydrogel. HCT is a potent corticosteroid with high efficacy and minimal side effect profile used in the management of inflammatory skin diseases. Currently, there is no literature showing the investigation of CMC hydrogel loaded with HCT used as potential thermo-responsive polymeric drug delivery system for topical drug delivery in PV. This drug delivery system has high therapeutic potential for sustained drug release in the epidermis accompanied by moisturizing effect and accepted by patients.

CHAPTER 3. DESIGN AND SYNTHESIS OF A TRANSDERMAL ANTI-PSORIATIC HYDROGEL FOR THE TREATMENT OF PSORIASIS VULGARIS

3.1 Introduction

Chronic inflammatory skin diseases are medicated by complex immunological mechanisms. In Psoriasis, the hyperproliferation of keratinocytes triggers an immune response leading to the release of cytokines (Xu *et al.*, 2021; Ni and Lai, 2020). Presently, there is no known cause for this disease as it can be triggered by a plethora of factors. Psoriasis affects up to approximately 5% of the world population and has been declared as a serious non-communicable disease by the World Health Organization (Grozdev and Korman, 2021). Psoriasis vulgaris (PV) is the most prevalent form of this disease accounting for 90% of all psoriasis diagnoses. The clinical presentations of PV include scaly itching, oedema, fatigue, burning, and erythema. In addition to the physical manifestations, this disease has also been linked with decline in mental state leading to thoughts of suicide and overall deterioration in quality of life (Maqbool *et al*., 2021; Armstrong and Read, 2020). Current treatment interventions for PV include topical corticosteroids, phototherapy, and systemic therapies based on the severity of the disease.

South African treatment guidelines state corticosteroids as a standard of care for this disease (Jacobs and Kgokolo, 2020; Steinhoff *et al*., 2020). Hydrocortisone (HCT) is a class V-VII, low-to-intermediate-potency corticosteroid with anti-pruritic, anti-inflammatory, and vasoconstrictive effects. HCT promotes suppression of the immune and inflammatory responses and is indicated for use (topically) in the treatment of various skin diseases, including PV. Currently, HCT is prescribed in the form of ointments, creams, and lotions for relief of PV symptoms. These HCT formulations show efficacy as therapeutic agents against PV; however, they are associated with undesirable local and systemic side effects, such as skin atrophy, pruritus, erythema, skin dryness and suppression of the Hypothalamus-Pituitary-Adrenal gland (HPA) axis ("Drugs.com", 2021). Other factors contributing to the limited utilization of topical corticosteroids are: lack of compliance by patients, frequent application of the medication, cost and availability of the medication, and lack of adequate knowledge about the disease (Gold *et al*., 2021; Svendsen *et al*., 2020). In this study HCT was employed as model anti-psoriatic drug for the treatment of PV.

To overcome challenges of patient compliance as well as to safeguard against undesirable side effects of HCT, novel and efficacious drug delivery systems should be investigated. Novel transdermal drug carriers have been evaluated for enhancing skin penetration of corticosteroids exemplified by microemulsion, hydrogel, niosomes, liposomal hydrogel, deformable liposomes and solid lipid nanoparticles (SLNs) (Altamimi *et al*., 2019; Giri, 2019.

The purpose of this study was to synthesise hydrocortisone (HCT) loaded (Sorbitan monostearate/SMS)-polycaprolactone (PCL) lipid nanoparticles encapsulated with Carboxymethyl cellulose (CMC) hydrogel base to form a hydrogel which is responsive to temperature (body temperature 37 ºC), pH (skin pH ~5.2) for improved transdermal treatment of Psoriasis Vulgaris (PV). The HCT loaded PCL nanoparticles were composed of lipid core so called lipid core-nanocapsule suspensions and were prepared by the interfacial polymer deposition method following solvent displacement and synthesis confirmed by physicochemical properties including Scanning Electron Microscopy (SEM), Fourier Transformation Infrared Spectroscopy (FTIR), zetasizer, Ultraviolet/Visual (UV/Vis) spectroscopy, Thermogravimetric Analysis (TGA) and Differential Scanning Calorimeter (DSC) for thermoanalysis. HCT-loaded PCL nanoparticles as well as HCT-PCL nanoparticles encapsulated with CMC gel (hydrogel) were dissolved in two different pH environments (pH 5,2 and pH 5,9) to simulate PV-infected and normal skin pH, respectfully. Furthermore, keratinocyte skin cells were treated with HCT-loaded PCL nanoparticles and evaluated for cytotoxicity utilising a 3-(4,5-dimethylthiazole-2-yl)-2,5-diphenyltetrazolium bromide dye (MTT) assay and absorbance measured at 570 nm employing a Thermo Lab systems Multiskan MK3 microplate reader.

3.2 Materials and Methods

3.2.1 Materials and Equipment

The following chemicals were sourced and utilized throughout this study: acetone, ethanol, methanol, Hydrocortisone (HCT), sorbitan monostearate (SMS), polysorbate 80 (Tween 80), distilled water (dH_2O), hydrochloric acid (HCl), stearic acid, oleic acid, sodium hydroxide (NaOH), Carboxymethyl Cellulose (CMC), Trypan blue dye, polycaprolactone (PCL), phosphate buffered saline (PBS), Dulbecco's Modified Eagle's Medium (DMEM), Trypsin, Dimethyl sulfoxide (DMSO), dimethylimidazole diphenyl tetrazolium bromide (MTT), and

mannitol. All chemicals utilized were sourced from Sigma-Aldrich and were of high analytical and experimental grade.

Nanophotometer [Implen™ NanoPhotometer™ NP80 UV/Vis Spectrophotometer (Munich, Germany)], DSC [Mettler Toledo, DSC1, STARe Instrument (Schwerzenback, Switzerland)], FTIR [PerkinElmer Spectrum 100, Beaconsfield, United Kingdom], TGA [PerkinElmer TGA 4000, Beaconsfield, United Kingdom], Zeta sizer [Zeta-sizer Nano-ZS machine (Malvern Instruments, Worcestershire, United Kingdom)], sonicator [Scientech Ultrasonic Cleaner, Labotec, South Africa], lyophilizer [FreeZone® 2.5, Labconco®, Kansas City, MS, USA], incubator (RS Biotechnological Galaxy, Irvine, UK), inverted light microscope, Model CKX53 (Olympus, Tokyo, Japan).

3.2.2 Spectrophotometric Determination of λ_{max} of HCT and Calibration Curve

The standard solution of HCT was prepared by creating a 10 mg/mL stock solution. Briefly, 100 mg of HCT was weighed and dissolved in 10 mL 50% ethanol solution as solvent. The mixture was sonicated for 10 minutes to ensure HCT is fully dissolved and labelled as primary stock solution. A secondary stock solution was prepared by further diluting 1 mL of the primary stock solution into 100 mL of the 50% ethanol solution to achieve a final concentration of 100 µg/mL.

Determination of the linear range (calibration curve) was done using standard solutions of the HCT drug at varying concentrations. The sample concentrations ranged from 1 µg/mL – 10 µg/mL. The samples were loaded into cuvettes and analysed utilizing a Implen™ NanoPhotometer™ NP80 UV/Vis Spectrophotometer (Munich, Germany). The concentration values used were 1 µg/mL, 3 µg/mL, 5 µg/mL, 8 µg/mL, and 10 µg/mL. Each sample was analysed in triplicate at $\lambda_{max.}$ To blank the spectrophotometer, the 50% ethanol solution was used. The averages (n = 3) of the resulting absorbance readings were recorded in the calibration curve given in **Figure 3.3** (Abbas *et al.*, 2017).

3.2.3 Synthesis of the SMC-PCL Nanoparticle Carrier System

Synthesis of the SMS-PCL nanoparticles was performed using a microemulsion technique wherein the hydrophobic corticosteroid HCT was encapsulated within a micelle structure (lipid core). Microemulsions are a system of oil, water, and surfactant. This technique yields isotropic, thermodynamically-stable, and translucent drug- nanoparticle dispersions (Gradzielski *et al*., 2021). This was performed as described by Da Silva *et al*. (2013) and Bender *et al*. (2012). The organic phase was created by accurately weighing 100 mg PCL, 20 mg HCT, and 38 mg SMS dissolved in 25 mL acetone under magnetic stirring at 37 °C until fully dissolved. Separately, an aqueous phase was created by slowly adding Tween 80 up to a final volume of 3 mL into 50 mL water under continuous magnetic stirring until homogenized. Both solutions were combined and left for 10 minutes under magnetic stirring at room temperature. The same procedure was followed to create the control sample for this study (SMS-PCL Blank). The acetone and excess water were removed by rotary evaporation and air drying to concentrate the nanoparticle samples. A final volume of 25 mL of both the HCT-loaded SMS-PCL nanoparticles and Blank SMS-PCL nanoparticle samples, respectively, was obtained. The obtained solutions were divided evenly into petri dishes and stored at -80 °C for 24 hours. To preserve the samples, a 5% (w/v) solution of mannitol was created and added in a 1:1 ratio with the nanoparticle samples.

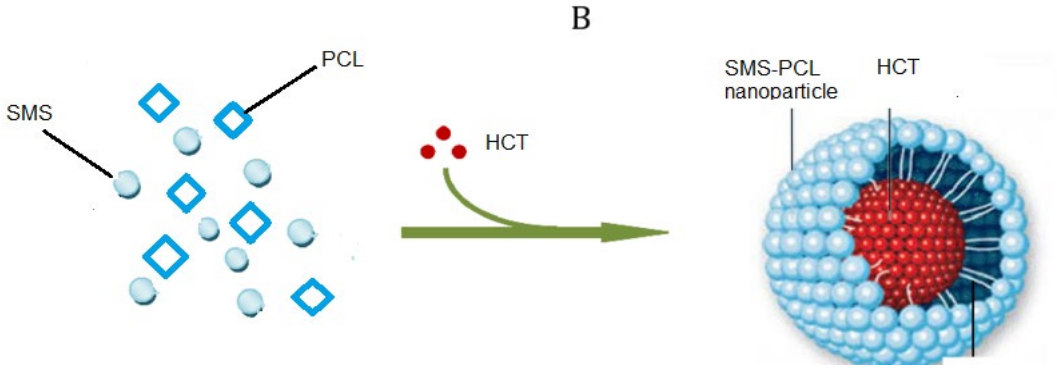


Figure 3.1 Illustration of the microemulsion method. The figure demonstrates loading of HCT into a micellar structure (SMS-PCL nanoparticle) for loading into the hydrogel (Image obtained from Güngör et al. (2015) with modification).

Finally, the samples were lyophilized employing a FreeZone® 2.5, Labconco® (Kansas City, MS, USA) lyophilizer for 24 hours at -80 °C to remove any excess water and yield a powder, which was subsequently stored at room temperature throughout the experiment.

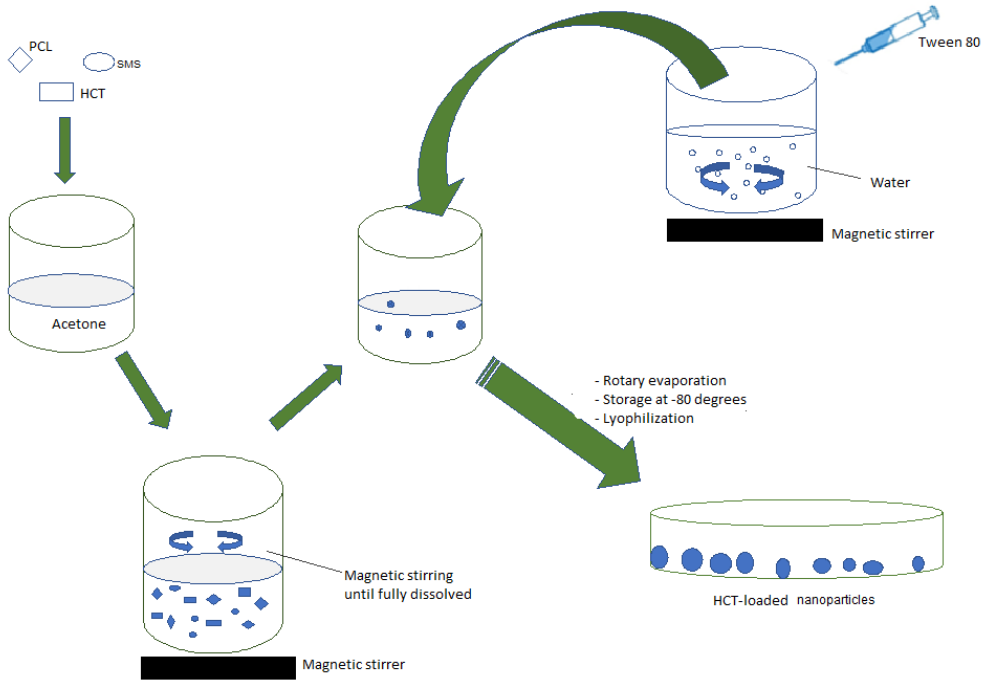


Figure 3.2: Schematic representation of the synthesis process for the HCT-loaded SMS-PCL nanoparticles.

3.2.4 Physical Assessment of the SMS-PCL Nanoparticles in Terms of Size, Stability, and Charge Distribution

The size, stability, and polydispersity index (PdI) the nanoparticles were determined using a Zeta-sizer Nano-ZS machine (Malvern Instruments, Worcestershire, United Kingdom). Briefly, 5 mg of each lyophilized sample was dissolved in distilled water and filtered through 0.22 µm syringe filter (Millipore Corp., Bedford, MA, USA). The samples were transferred to cuvettes and sonicated to ensure complete dissolution. The analyses were performed in triplicates. All readings were performed at 25 °C. Results were obtained using dynamic light scattering (Dehkharghani *et al*., 2018; Pantshwa *et al*., 2017) and recorded in **Figure 3.4**.

3.2.5 Determination of the Drug Entrapment Efficacy of HCT within the SMS-PCL Nanoparticles

The Drug Entrapment Efficacy (DEE) of HCT within the SMS-PCL nanoparticles was determined using an indirect method. In short, the SMS-PCL nanoparticle dispersions (both drug-loaded and blank) were placed in centrifuge tubes and centrifuged at 12 000 rpm for 45

minutes. The supernatant was carefully withdrawn without disturbing the pallet and diluted utilising a 50% ethanol solution (at a 1:9 [v/v] ratio). The samples were analysed from the calibration curve utilizing a Implen™ NanoPhotometer™ NP80 UV/Vis Spectrophotometer (Munich, Germany) at wavelength 245 nm making use of the SMS-PCL Blank loaded supernatant as the blank. To determine the DEE of HCT within the nanoparticles, **Equation 1** was used (Avasatthi *et al*., 2016; Khurana *et al*., 2013):

$$DEE\ (\%) = \frac{[Drug]_{after\ loading}}{[Drug]_{before\ loading}} x100$$

Equation 1 Drug Entrapment Efficacy (DEE) calculation of HCT within the SMS-PCL nanoparticles

3.2.6 Chemical Evaluation Undertaken on the SMS-PCL nanoparticles, HCT, and HCT-loaded nanoparticles

FTIR spectroscopy was carried out on the HCT, HCT-loaded nanoparticle and nondrug-loaded nanoparticles (SMS-PCL Blank) to compare and evaluate structural properties. FTIR spectra were recorded on a Perkin Elmer Spectrum 100 FTIR spectrometer (Llantrisant, Wales, UK), using an ATR-FTIR cell and a diamond crystal internal reflection element. Samples were analysed at a wavenumber range of 650 – 4000 cm^{-1} with a resolution of 4 cm^{-1} and 64 scans per spectrum. The resulting spectra were recorded.

3.2.7 Thermal Transition Evaluation of the SMS-PCL nanoparticles, HCT, and HCT-loaded nanoparticles

Comparative DSC analyses were performed on lyophilized samples of the HCT-loaded nanoparticles, HCT drug, and the Blank nanoparticle sample using a Mettler Toledo, DSC1, STARe System (Schwerzenback, Switzerland) at a heating rate of 10 °C/min from 0°C to 200 °C under a constant flow of N_2 gas. Accurately weighed samples (10-15 mg) were placed into a covered aluminium sample holder containing a central pin hole. Indium metal (99.99%) was used to calibrate the DSC modulus in relation to temperature and enthalpy. An empty sample holder was used as a reference. DSC thermograms were then compared for transitions.

3.2.8 Thermal Evaluation of the SMS-PCL nanoparticles, HCT, HCT-loaded nanoparticles

TGA was utilized to facilitate rapid degradation analysis by approximating the speed at which these samples become degraded and the specific heat at which this takes place. TGA was carried using the TGA software (PerkinElmer STA 6000, Beaconsfield, United Kingdom) to

elucidate the thermal characteristics of HCT, HCT-loaded nanoparticles, and Blank nanoparticle samples. Ten (10) mg of each sample was weighed accurately and placed on crucibles in preparation for analysis. Heating was undertaken from 30 °C to 900 °C at a rate of 10 °C/min under constant N_2 gas flow of 20 mL/min.

3.2.9 Synthesis and Evaluation of the CMC Hydrogel System

The method of synthesis of the hydrogel was adopted from Andonova et al. (2017). Briefly, CMC hydrogel was prepared by dissolving 2 g of CMC in 100 mL of boiling deionized water under slow magnetic stirring until the CMC was fully dissolved. Dropwise addition of NaOH was made until gelation occurred.

The temperature it takes for the hydrogel to reach sol-gel transition (SGTT) was determined using a tube inversion method. Briefly, 5 mL of the hydrogel formulation was placed in glass vials and heated in a water bath slowly (rate of 1 ºC/min) from 10 ºC to 40 ºC. The flowability of the hydrogel was observed at each time point by tilting the vial. The temperature at which the liquid is found to be immobile was recorded as the SGTT.

3.2.10 *In vitro* Drug Release Undertaken on the SMS-PCL nanoparticles, as well as the Loaded CMC Hydrogel

The *in vitro* release of HCT from the HCT-loaded SMS-PCL nanoparticles, as well as the hydrogel system was investigated using a dialysis method by weighing 40 mg of the HCT-loaded nanoparticles into a dialysis membrane (MW = 10000 kDa) pre-swollen in 50 mL of PBS (dissolution medium) at pH ~5.2 and pH ~5.9 - to simulate the PV infected skin and healthy skin environments, respectively (Shinde et al., 2020; Bigliardi, 2018). The nanoparticles were also added to 10 mg of the hydrogel to investigate the drug release of HCT from the thermo-responsive CMC hydrogel. Once loaded, the mixture was placed in an isothermal shaker (20 rpm) at 37 °C. Time intervals for sampling were determined and sampling was done over a period pf 24 hours. At each time point, 3 mL aliquots of the release medium were withdrawn and replaced with an equal volume of fresh medium. The concentration of HCT in the release medium was assayed by UV/Vis spectrophotometry (Implen™ NanoPhotometer™ NP80 UV/Vis Spectrophotometer, Munich, Germany) at wavelength 245 nm (Pantshwa *et al*., 2017; Khurana *et al*., 2013). All sampling was performed in triplicate for statistical significance. Calculations of the concentration of drug released were

performed utilizing the calibration curve and plotted in Figure 3.8 and Figure 3.9. To determine the mass of the drug released, and percentage thereof, **Equation 2** was used:

$$Mass\ of\ drug\ released\ (mg) = \frac{Concentration\ of\ drug \times volume\ of\ dissolution\ medium}{1000}$$

Equation 2 Calculation of mass of HCT released from the SMS-PCL nanoparticles as well as SMS-PCL nanoparticles encapsulated within the CMC hydrogel

3.2.11 Analysis of the Surface Morphology of the HCT-loaded Nanoparticles Using SEM

The shape and structure of the HCT-loaded nanoparticles was studied using Scanning Electron Microscopy (SEM) - JEOL 840 SEM (JEOL, Japan). The lyophilized samples will be fixed to a metal stub using conductive tape and the sputter coated with gold. This occurred under vacuum at 2 kV accelerating voltage. The resulting micrographs were evaluated and the surface morphology.

3.2.12 *In vitro* Cytotoxicity

3.2.12.1 Keratinocytes Culture Employing HaCaT Cell Lines

Cytotoxicity evaluation was conducted using the HaCaT cell lines. HaCaT cells are spontaneous, immortalized human keratinocyte model widely used in the study of skin diseases, including chronic inflammatory skin conditions (Colombo et al., 2017). The cells were cultured in Dulbecco's Modified Eagle's Medium (DMEM) growth medium, supplemented with 10% Foetal Bovine Serum (FBS) and 1% Penicillin-Streptomycin, to form a differentiated model of the human keratinocytes. The HaCaT culture was incubated at 37 °C and 5% CO_2 saturation under humid conditions (RS Biotechnological Galaxy, Irvine, UK) for 24 hours until confluence of >90% was reached, at which stage the cells were sub-cultured. The sub-culturing process was begun by removing growth medium and rinsing the cells with PBS. The cells were detached from the bottom of the T75 cell culture flask using Trypsin. The cells were left to trypsinize for 5 min at 37 °C and 5% CO_2. and transferred to flasks containing fresh growth medium.

3.2.12.2 Cell Morphology and Cell Count

The cells were observed for morphology and number using an inverted microscope. Subsequently, the cells were prepared for counting by diluting 0.5 mL of cells in 1 mL DMEM. From the resulting cell suspension, 10 µl was withdrawn and strained with trypan blue dye (1:1 v/v ratio). Counting was performed utilizing a haemocytometer. **Equation 3** was used to count the average number of viable.

$$No.of\ viable\ cells\ =\ Avg\ cells\ counted\ \times Dilution\ Factor\ \times 10^4\ cells/ml$$

Equation 3 Calculation of number of viable cells

where 10^4 is a constant with dilution factor being 6.

3.2.12.3 Standard Drug Preparation

Standard drugs/samples were prepared by dissolving pure HCT, HCT-loaded nanoparticles, and Blank nanoparticles in dimethyl sulfoxide (DMSO) to reach a final concentration of 20 mg/mL and 10 mg/mL for 5-fluorouracil (5-FU), respectively (stock solutions). 5-FU is an antineoplastic chemotherapeutic drug used as a positive control in this present study. All drugs were vortexed until dissolving completely and stored. The drug-loaded and blank hydrogels were prepared by loading 0.5 mL of the hydrogel (at room temp) with 0.5 mL of the HCT-loaded nanoparticles and 0,5 mL of the Blank nanoparticles, respectively, ensuring the two mix thoroughly.

All samples were serially diluted in PBS to achieve concentrations of 1,625 µg/mL, 3,25 µg/mL, and 6,5 µg/mL. Different concentration ranges were evaluated in order to establish a relationship between the toxicity of the drug and the cellular response. All drugs were stored under refrigeration conditions (5 ºC), covered in foil to prevent degradation by light for the duration of the study.

3.2.12.4 In vitro Cytotoxicity Assay Preparations

The HaCaT cells were seeded in a 96-well plate at a seeding density of 100,000 cells/mL. To each well, 90 µl of the cell suspension was added and incubated at 37 ºC, 5% CO_2 in a humidified atmosphere for 24 hours to ensure attachment of the cells to the plate. Samples were treated with 10 µl volumes, making final concentrations of 1.625, 3.25 and 6.5 µg/mL.

Following incubation, the cells were treated with 10 µl of the pure HCT, HCT-loaded nanoparticles, HCT-loaded hydrogel, and Blank hydrogel. Negative control samples included Blank nanoparticles, DMSO (at 0.03%), and untreated cells. For a positive control, cells were treated with 10 µg/mL of 5-Fluorouracil (5-FU). The treated cells were incubated for a further 24 hours. All treatments were performed in triplicates and reported as mean values.

3.2.12.5 MTT Cytotoxicity Assay to Determine the Safety and Tolerability of the HCT-loaded CMC Hydrogel

Methylthiazole Tetrazolium salt (MTT) is a colorimetric assay utilized to determine cytotoxicity and assessing cell viability (Kumar *et al*., 2018). The *in vitro* cytotoxicity of the thermo-responsive HCT-loaded hydrogel system was evaluated by employing this assay after 24- and 48-hour treatments. Briefly, following the 24-hour incubation period of the treated cells, the growth medium was removed and replenished with fresh medium (90 µl) and addition of 10 µl of the MTT solution (5 mg/mL) to each well. The 96-well plate was incubated for 4 hours following addition of MTT at 37 ºC and 5% CO_2 under humid conditions. The resulting formazan crystals that formed at the bottom of the plate were dissolved with 100 µl of the solubilizing agent and incubated overnight at 37 ºC and 5% CO_2. The following day, absorbances were recorded at 570 nm with a reference wavelength of 620 nm using a multimode microplate reader (Victor X3, Perkin Elmer, Massachusetts, USA). Mean values of the corrected absorbance measurements of each triplicate treatment were computed relative to the mean values of DMSO (0.03%) control (set at 100% viability).

The cell viability (%) for each drug concentration was calculated the following equation:

$$Cell\ viability\ (\%) = \frac{Absorbance\ (Test)}{Absorbance\ (Control)} \times 100$$

Equation 4 Cell viability calculation following MTT Assay

Where *Absorbance* is the mean absorbance (n = 3) recorded for different drug concentrations and DMSO (0.03%) is taken as used as the control.

3.2.12.6 Light Microscopy Analysis to Evaluate Internalization of the Therapeutic Compounds Within the HaCaT Cells

The internalization of the HCT-loaded SMS-PCL nanoparticles, HCT-loaded CMC hydrogel, Plain hydrogel, SMS-PCL nanoparticles (blank), Pure HCT, PBS, DMSO, and 5-FU into the HaCaT cells was determined microscopically. Briefly, after 48 hours of treatment, the images were captured using an inverted light microscope, Model CKX53 (Olympus, Tokyo, Japan) using the 10X objective. The resulting images were recorded and presented in the Results section.

3.3 Results and Discussion

3.3.1 Spectrophotometric Analysis Undertaken to Determine λ_{max} of HCT and Calibration Curve

The λ_{max} of HCT was found at 245.0 nm. Based on the λ_{max}, the calibration curve was obtained (**Figure 3.3**). This curve confirms that there is a linear correlation between concentration of the drug and the absorbance (R^2 = 0,9994) – i.e., an increase in the concentration of the drug results in an increase in the respective absorbance (Abbas *et al*., 2017).

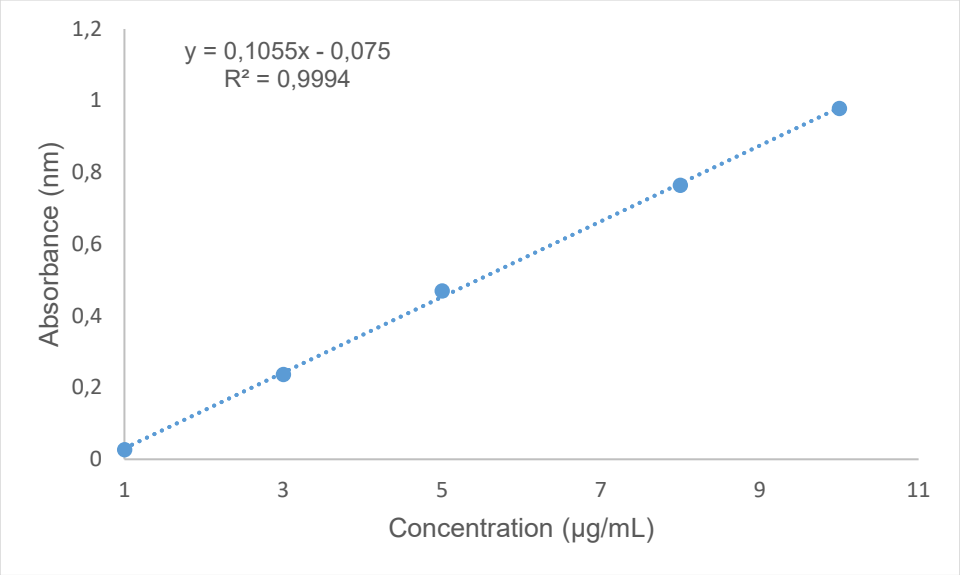


Figure 3.3 Calibration curve of HCT.

3.3.2 Physical Assessment of the SMS-PCL Nanoparticles in Terms of Size, Stability, Charge Distribution, And Drug Entrapment

The HCT-loaded as well as blank mean nanoparticle sizes were found to be 110.5 nm and 77.9 nm with PdI of 0.15 and 0.22, respectively. The loading of HCT into the nanoparticles resulted in larger diameter of the NLC. The mean zeta potential for the HCT-loaded nanoparticles obtained was -58.7 mV.

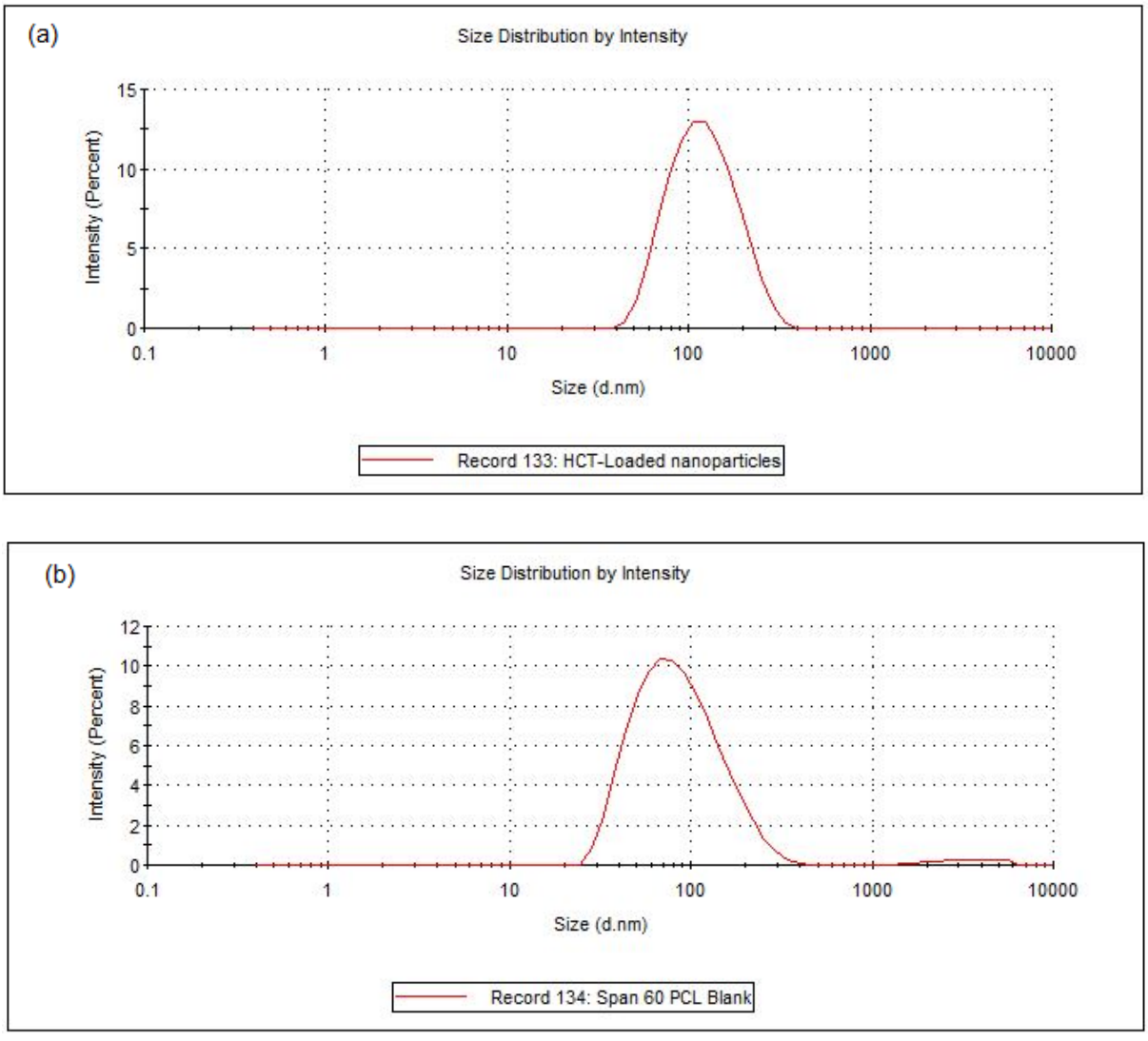


Figure 3.4 Nanoparticle size of (a) HCT-loaded and (b) SMS-PCL Blank nanoparticles

substances such as corticosteroids within hydrogels. The size of the nanoparticles is critical to the biological function of these nanoparticles. In the case of drug delivery across the skin (transdermal drug delivery), the optimum particle size for drug delivery to the deep layers of the skin is noted to be <200 nm in diameter (Danaei *et al*., 2018). The HCT-loaded nanoparticles were found to be 110.5 nm in diameter, thus making them effective transdermal drug delivery platforms. The zeta potential of nanostructures is a key indicator of the stability of colloidal nanostructure dispersions. The mean zeta potential of the HCT-loaded nanoparticles (-58.7 mV) indicates that the nanoparticles have excellent long-term stability ("nanoComposix", 2021). The PdI values recorded for both the HCT-loaded and blank nanoparticles (PdI <0.5) show that the distribution of the nanoparticle size is of a homogenous nature (Pantshwa *et al*., 2017).

The DEE of the HCT-loaded nanoparticles was found to be 76% (only 24% of the initial concentration of the drug was recovered in the supernatant). Thus, the microemulsion technique proved to be an effective technique for loading HCT in lipid carriers.

3.3.3 Chemical Evaluation Undertaken on the SMS-PCL nanoparticles, HCT, and HCT-loaded nanoparticles

FTIR spectra for HCT, HCT-loaded nanoparticles, and blank (SMS-PCL) samples were obtained and recorded in **Figure 3.5**.

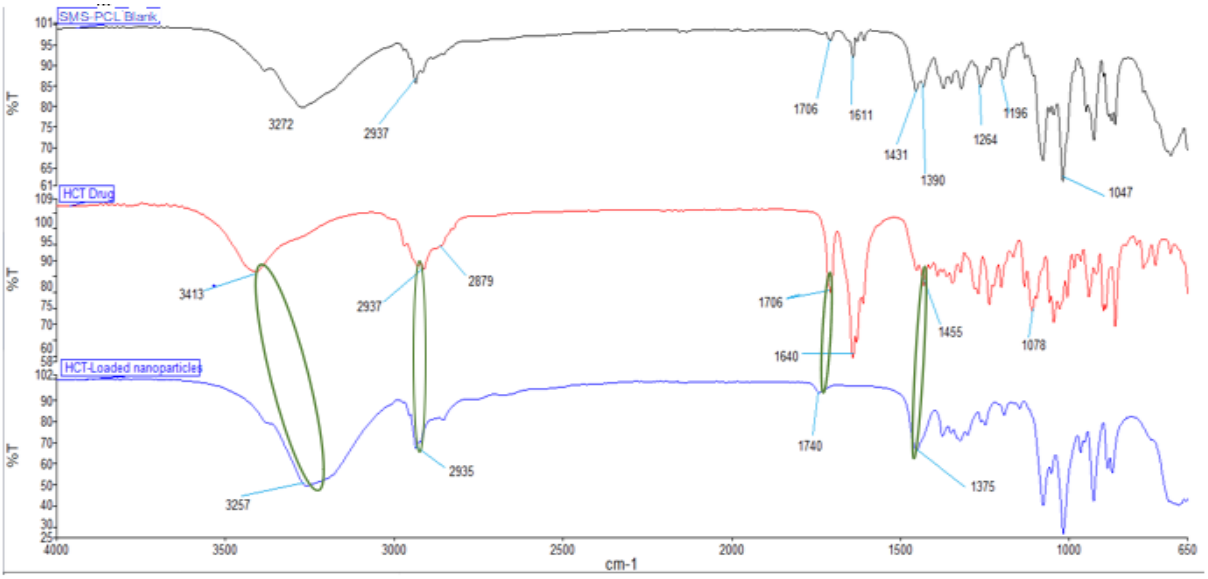


Figure 3.5 FTIR Spectra of the SMS-PCL Blank polymers, HCT drug (pure), and HCT-loaded nanoparticles.

The IR spectrum of HCT showed distinct peaks at 3413 cm^{-1}, which confirms the presence of –OH groups, aliphatic C–H stretching was observed at 2937 cm^{-1} as well as 2879 cm^{-1}, C=O was observed at 1706 cm^{-1} and 1640 cm^{-1}, –CH2 bending was seen at 1455 cm^{-1}, lasty the

spectrum showed C–O at 1078 cm^{-1} (Huang *et al.*, 2020; Dehkharghani *et al*., 2018). In the spectrum for the SMS-PCL blank, the peak observed at 2937 cm^{-1} is due to CH_2 vibrations, the peak at 1706 cm^{-1} is due to C=O vibrations, the peak at 1611 cm^{-1} represents O-H vibrations, while vibrations caused by CH_2 can be observed at the 1431 and 1390 cm^{-1} peaks, C-O and C-C stretching vibrations can be observed at 1264 cm^{-1}, and 1196 cm^{-1}, respectively, and 1047 cm^{-1} shows COO vibrations (Fatehi *et al*., 2020; Chakrapan *et al.*, 2012; Elzein *et al*., 2004).

With regards to the FTIR spectrum of the drug-loaded nanoparticles, changes in concavity and intensity of the peaks denotes interaction of the drug with the polymers. In this instance this interaction was observed at peaks 3257 cm^{-1} where the O-H group of HCT interacts with the polymer matrix (Nandiyanto *et al*., 2019). At 2935 cm^{-1}, the spectrum denotes long-chain linear aliphatic compounds (SMS) interaction with HCT, followed by more interactions at 1740 cm^{-1}, and 1375 cm^{-1}, respectively.

3.3.4 Thermal Transition Evaluation of the SMS-PCL nanoparticles, HCT, and HCT-loaded nanoparticles

Comparative DSC analyses were performed on all samples. The thermograms obtained were recorded in **Figure 3.6**. In the figure, an endothermic peak can be observed at 200 °C, this corresponds with the melting point of HCT at 22 min; this can be corroborated as within the normal melting range of this drug (200 °C – 220 °C) per the literature (Altamimi *et al*., 2019; Ali *et al*., 2009; Cavalli et al., 1999) and confirmed by TGA data. The HCT melting peak is not observed within the polymer, suggesting that this compound is in an amorphous state, further supporting the fact that it has integration within the SMS-PCL nanoparticulate structure (Ali *et al*., 2009). The SMS-PCL nanoparticles demonstrated a sharp peak at 150 °C after 17 mins. No secondary peaks were observed, suggesting that the structure melted completely at this temperature (Awasthi *et al.*, 2021; Witika *et al*., 2021).

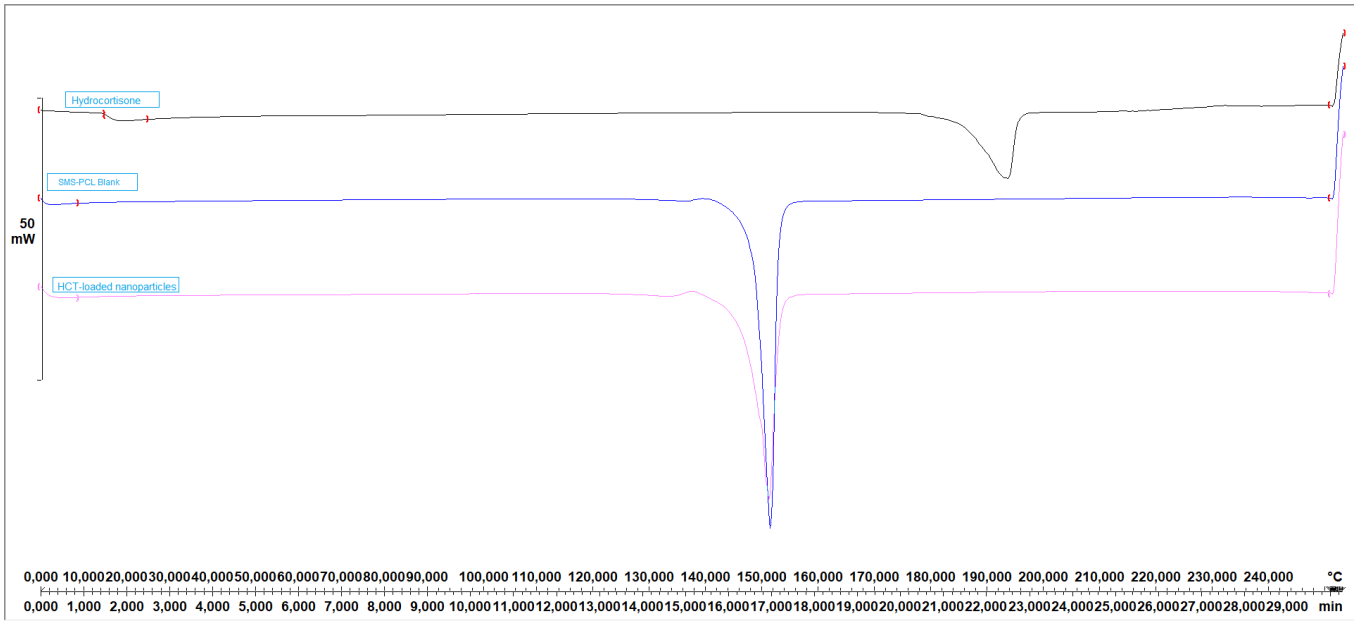
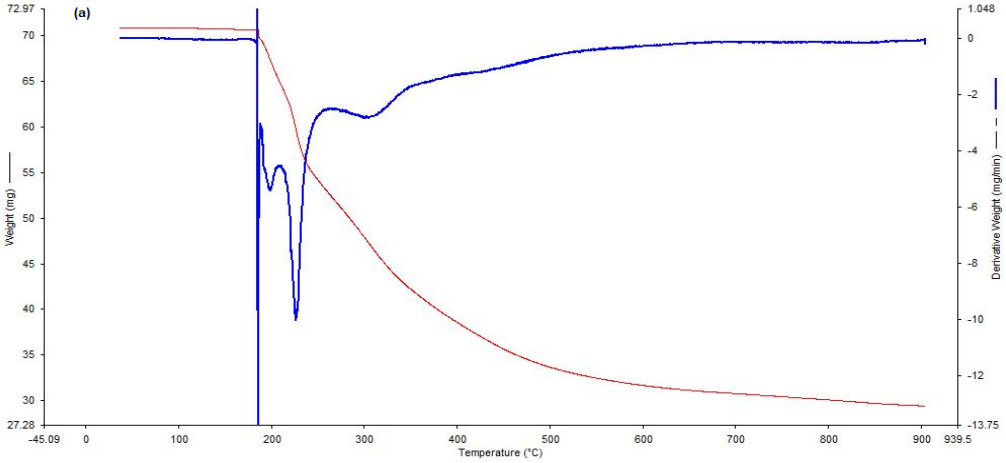
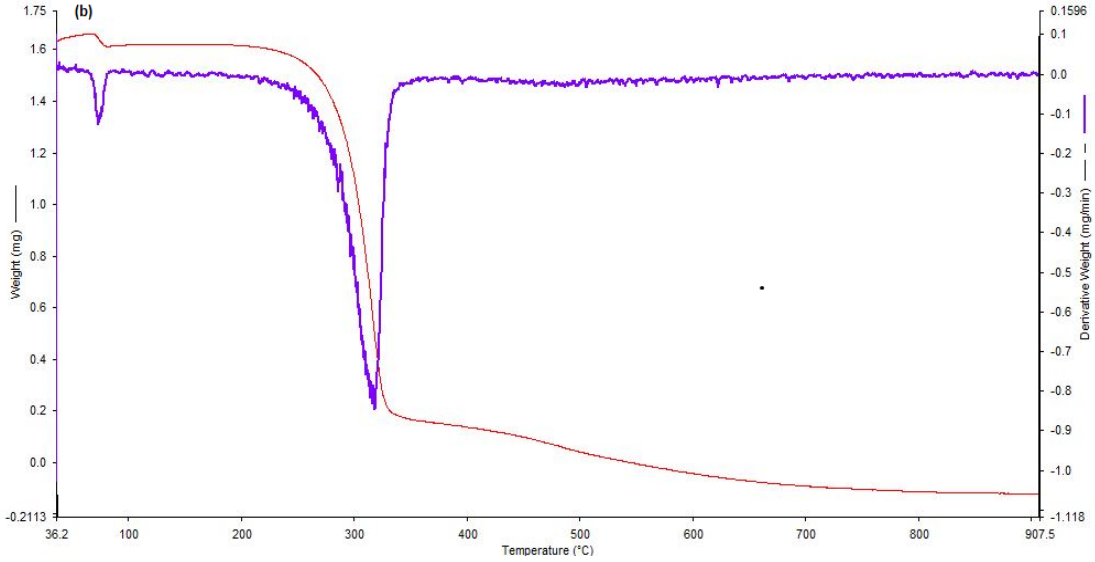


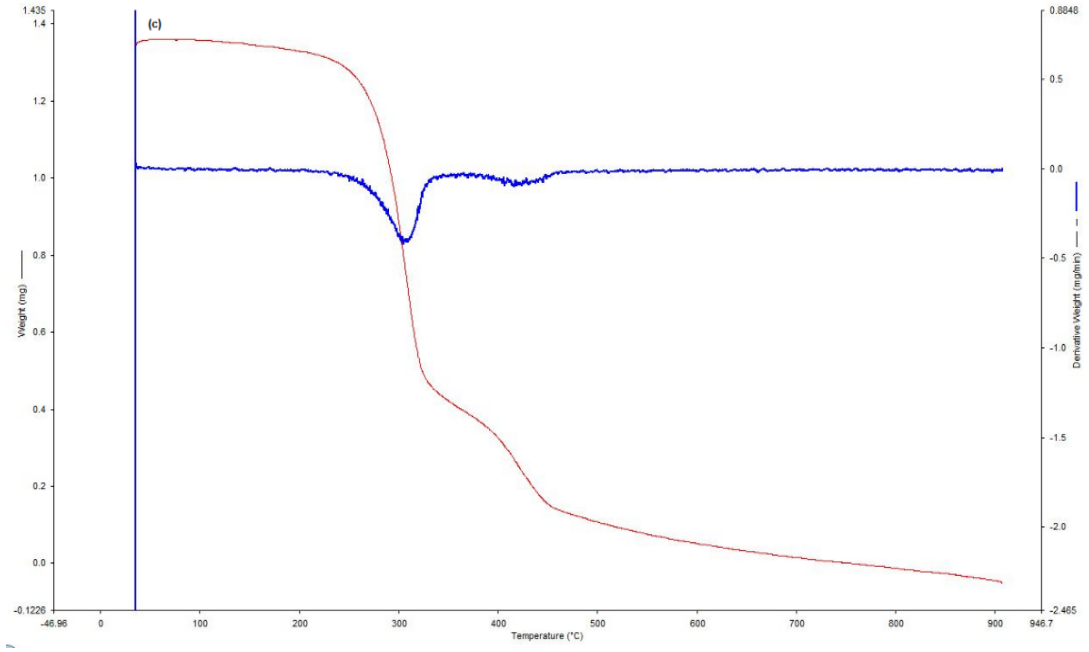
Figure 3.6 DSC of HCT, SMS-PCL Blank, and HCT-loaded nanoparticles.

3.3.5 Thermal Evaluation of the SMS-PCL nanoparticles, HCT, HCT-loaded nanoparticles

Figure 3.7 shows the TGA thermograms of pure HCT drug, SMS-PCL blank nanoparticles, as well as HCT-loaded nanoparticles. The derivative weight (mg/min) peaks represent critical temperatures in which loss of mass and decomposition occur. With regards to the pure HCT drug thermogram (**Figure 3.7(a)**), three critical weight loss stages can be observed at 220 °C (onset of decomposition), 305 °C (major decomposition), and, lastly, the maximum degradation of HCT is seen at 630 °C. In **Figure 3.7(b)**, the SMS-PCL blank samples show mass loss around 60 °C which could be as a result of evaporation of organic solvents and water weight. The polymer shows onset of degradation at approximately 290 °C and maximum decomposition between 320 °C and 500 °C. The HCT-loaded nanoparticles (**Figure 3.7(c)**) exhibit similar thermal behaviour to the blank nanoparticles. In the HCT-loaded thermogram, the degradation of HCT drug was not observed (Voss *et al*., 2020; Barrera-Rivera *et al*., 2018; Mendelson-Mastey *et al*., 2017).


(a)
Weight (mg)
Derivative Weight (mg/min)
Temperature (°C)


(b)
Weight (mg)
Derivative Weight (mg/min)
Temperature (°C)


(c)
Weight (mg)
Derivative Weight (mg/min)
Temperature (°C)

3.3.6 Evaluation of the CMC Hydrogel System for Sol-Gel Transition Temperature

The CMC hydrogel was successfully synthesized. A clear, translucent fluid was obtained. The SGTT was determined using a tube inversion method. With increasing temperature, the viscosity of the gel increased. The SGTT was determined at ~33 ºC±2 ºC. At room temperature, the hydrogel reverts to liquid consistency.

This confirms the successful synthesis of a polymeric thermo-responsive hydrogel system capable of delivery of drugs at physiological temperatures.

3.3.7 *In vitro* Drug Release Undertaken on the SMS-PCL nanoparticles, as well as the Loaded CMC Hydrogel

The drug release profiles of HCT from nanoparticles, as well as nanoparticle-loaded hydrogel were determined by analysis of the release medium at pre-determined time points (**Table 3-1** and **Table 3-2**) over a period of 24 hours. Overall, the HCT drug release from the thermo-responsive CMC hydrogel was slower as compare to the drug release from the nanoparticles at both pH environments. This could be as a result of slow diffusion of the drug across the polymer matrix; this is further evidence of the sustained drug release of HCT across the CMC hydrogel (Avasatthi *et al*., 2016). The maximum concentration of release was observed to be 3,25 µg/mL (0,84% release), this could be attributed to the PCL polymer's ability to hold onto hydrophobic compounds, such as HCT. The SMS-PCL nanoparticles encapsulated with CMC hydrogel demonstrated slow and sustained and controlled release of HCT (Rosado *et al.,* 2013; Lee *et al*., 2005). The CMC hydrogel further archived minimal absorption of HCT when applied via the topical route (Rosado *et al.,* 2013). This is key in preventing adverse reaction experienced with high concentration of HCT (Palmer and DeLouise, 2016). This is further exemplified by currently available formulations of the HCT (cream, oitments) having low drug percentage (usually 0,1% to 0,5%) (Armstrong and Read, 2020).

It has also been observed that the HCT drug releases at a faster rate at higher pH (5,9) - which is closer to physiological pH - compared to the low pH for both the nanoparticles and hydrogel formulations (Katas *et al*., 2012; Lee *et al*., 2005). The results are presented as mean ± SD (n = 3).

3.3.8 Analysis of the Surface Morphology of the HCT-loaded Nanoparticles Using SEM

The results of the SEM analysis demonstrated spherical shapes of the nanoparticles. This confirms that the HCT-loaded nanoparticles were synthesised and have polymeric structure as shown in **Figure 3.8** (Mahmoudi *et al*., 2020). This further validated that the hydrophobic drug, HCT, was successfully incorporated within the nanoparticle structure. Additionally, the spherical structure shows self-aggregation of the polymer molecules – i.e. the hydrophilic "heads" of the polymer molecules face outside, while the hydrophobic "tails" are shielded inside the core of the micelle – thus shielding contents of the micelle from the aqueous environment of the hydrogel (Nastili *et al*., 2017).

Furthermore, this nanoparticle structure offers considerable advantage in terms of topical delivery. Nanoparticle structures enhance stratum corneum permeation due to their lipophilicity, are small enough to cross the skin barrier (<200 nm), and have high stability, as well as high therapeutic activity (Danaei *et al*., 2018; Nastili *et al*., 2017). This firmLy places the synthesised SMS-PCL nanoparticles as excellent drug delivery vehicles for the topical delivery of HCT in the treatment of PV.

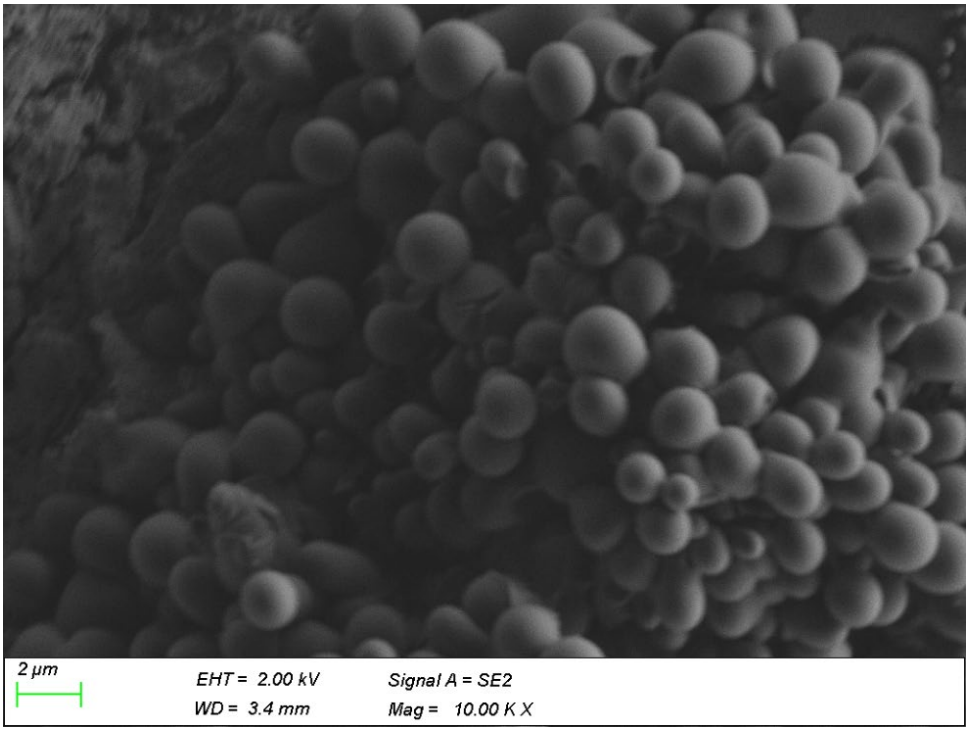


Table 3-1 HCT Drug Release Profiles at pH 5.2

HCT-loaded Nanoparticles				
Time (Hrs)	**Absorbance (nm)**	**Concentration (µg/mL)**	**Mass (mg)**	**Percentage (%) release**
0	0,042±0,004	0,837	0,046	0,230
0.25	0,065±0,004	1,067	0,059	0,293
0.5	0,071±0,004	1,123	0,062	0,309
1	0,085±0,003	1,262	0,069	0,347
2	0,101±0,003	1,420	0,078	0,390
4	0,186±0,004	2,263	0,124	0,622
6	0,215±0,007	2,546	0,140	0,700
24	0,250±0,009	2,899	0,159	0,797

HCT-loaded CMC Hydrogel				
Time (Hrs)	**Absorbance (nm)**	**Concentration (µg/mL)**	**Mass (mg)**	**Percentage (%) release**
0	0.013±0,002	0,557	0,031	0,153
0.25	0,056±0,002	0,975	0,054	0,268
0.5	0,062±0,002	1,038	0,057	0,285
1	0,081±0,001	1,222	0,067	0,336
2	0,093±0,004	1,347	0,074	0,370
4	0,172±0,003	2,128	0,117	0,585
6	0,190±0,002	2,299	0,126	0,632
24	0,242±0,002	2,813	0,155	0,774

Table 3-2 HCT Drug Release Profiles at pH 5.9

HCT-loaded Nanoparticles				
Time (Hrs)	**Absorbance (nm)**	**Concentration (µg/mL)**	**Mass (mg)**	**Percentage (%) release**
0	0.053±0,002	0,945	0,052	0,260
0.25	0,079±0,007	1,202	0,066	0,331
0.5	0,102±0,004	1,433	0,079	0,394
1	0,132±0,002	1,729	0,095	0,476
2	0,185±0,005	1,256	0,124	0,620
4	0,203±0,003	2,428	0,134	0,668
6	0,229±0,005	2,691	0,148	0,740
24	0,286±0,005	3,248	0,179	0,839

HCT-loaded CMC Hydrogel				
Time (Hrs)	**Absorbance (nm)**	**Concentration (µg/mL)**	**Mass (mg)**	**Percentage (%) release**
0	0.053±0,002	0,945	0,047	0,236
0.25	0,079±0,007	1,202	0,063	0,313
0.5	0,102±0,004	1,433	0,071	0,356
1	0,132±0,002	1,729	0,093	0,465
2	0,185±0,005	1,256	0,099	0,494
4	0,203±0,003	2,428	0,127	0,633
6	0,229±0,005	2,691	0,141	0,707
24	0,286±0,005	3,248	0,164	0,819

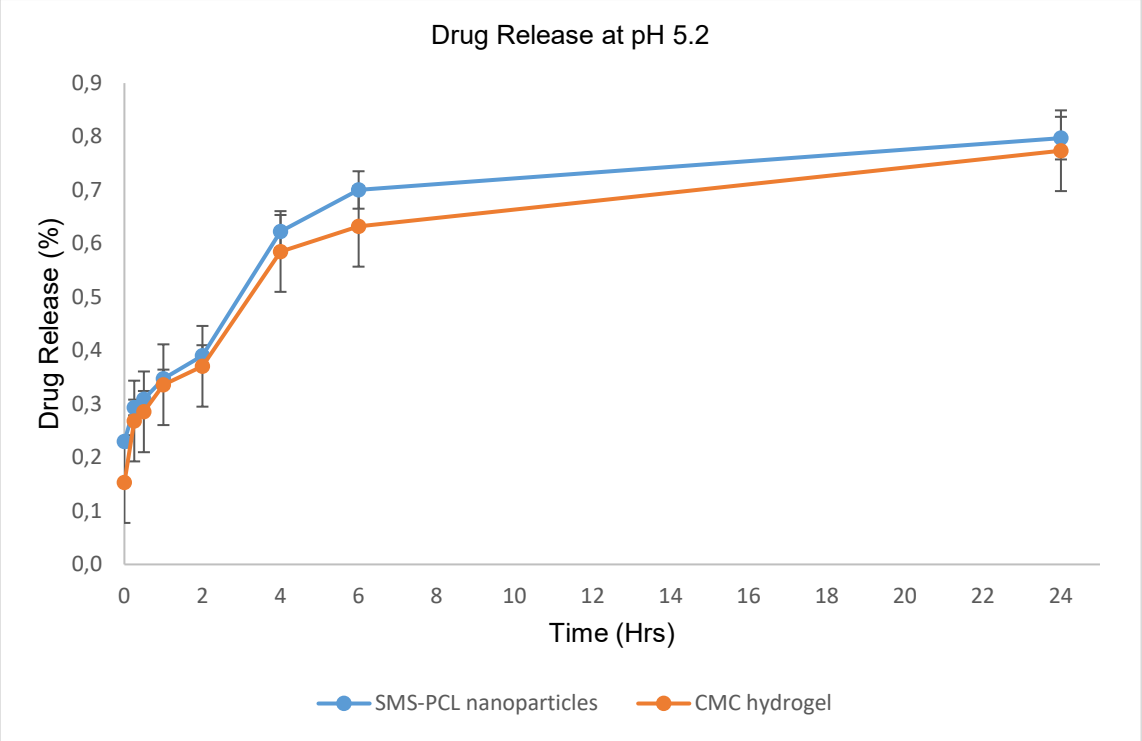


Figure 3.9 HCT release profiles from SMS-PCL nanoparticles and CMC hydrogel at simulated PV skin pH (pH 5.2) at 37 ºC over a period of 24 Hrs.

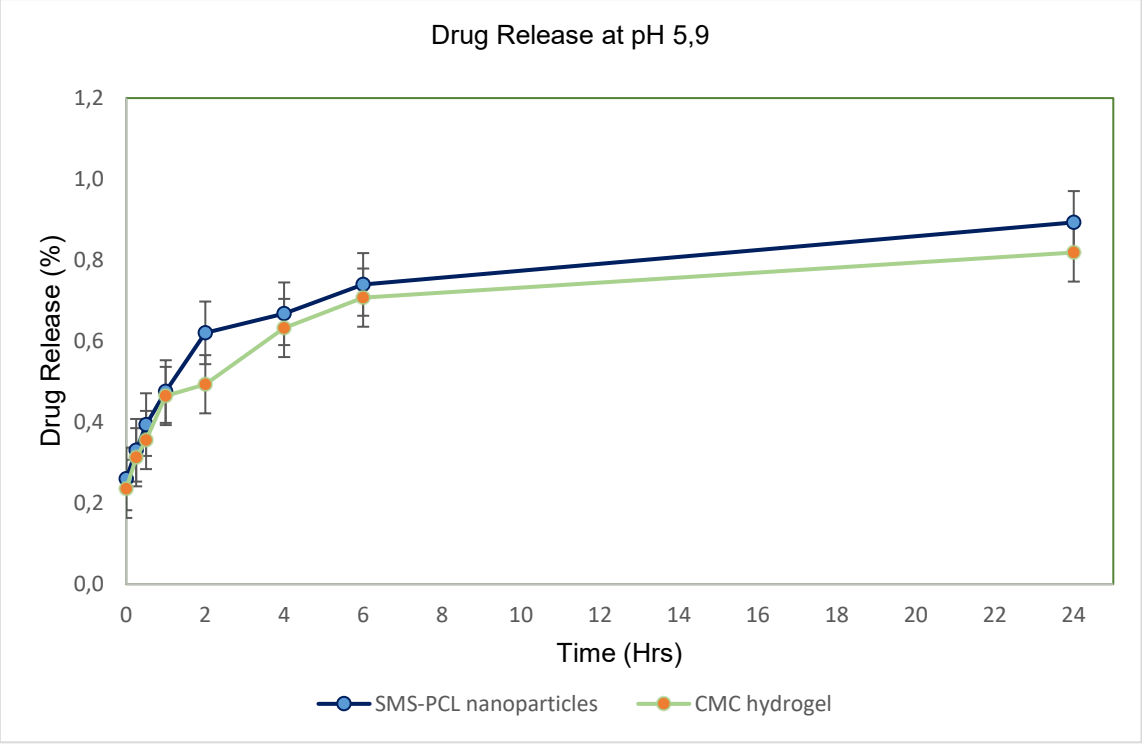


Figure 3.10 HCT release profiles from SMS-PCL nanoparticles and CMC hydrogel at simulated normal skin pH (pH 5.9) at 37 ºC over a period of 24 Hrs.

3.3.9 In vitro Cytotoxicity

In order to determine the safety and applicability of the thermo-responsive HCT-loaded hydrogel, cytotoxicity evaluations were conducted. In this study, the MTT assay data of the Plain hydrogel, HCT-loaded hydrogel, Pure HCT, HCT-loaded nanoparticles, and Blank nanoparticles was collected at 24- and 48 hours and depicted in **Figure 3.11** and **Figure 3.12**, respectively. The viability of the treated cells at both time points were maintained. At 24 hours (3,25 µg/mL), the viability of the HCT nanoparticles was and 95%, whereas the HCT-loaded hydrogel showed viability of 89%, respectively, when compared against the positive control (5-FU) at 80%. After 48 hours, the HCT-loaded nanoparticles and HCT-loaded hydrogel had high viability (116% and 124%, respectively at 3,25 µg/mL) vs 5-FU (46%). The loaded hydrogel demonstrated a slight decrease in cell viability when compared to the HCT nanoparticles alone.

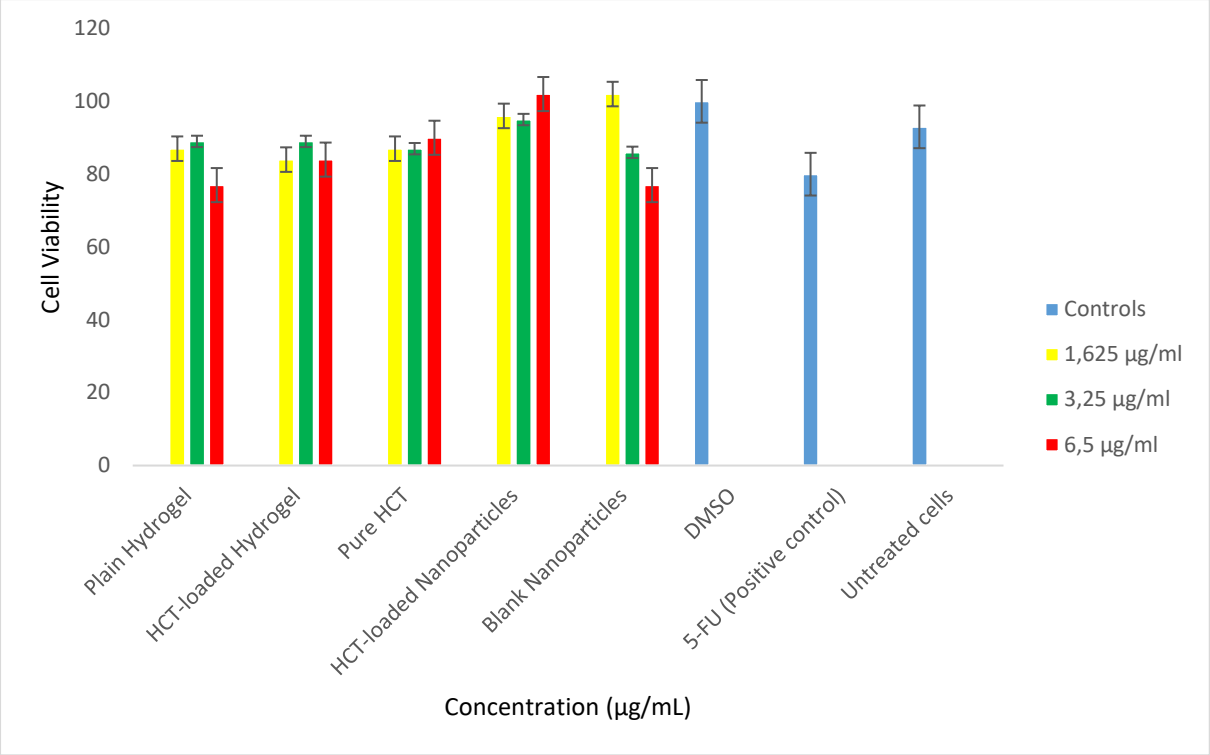


Figure 3.11 HaCaT Cell Viability (%) following treatment after 24 hours. The graph shows cell viability following MTT Assay of the treated cells against the controls.

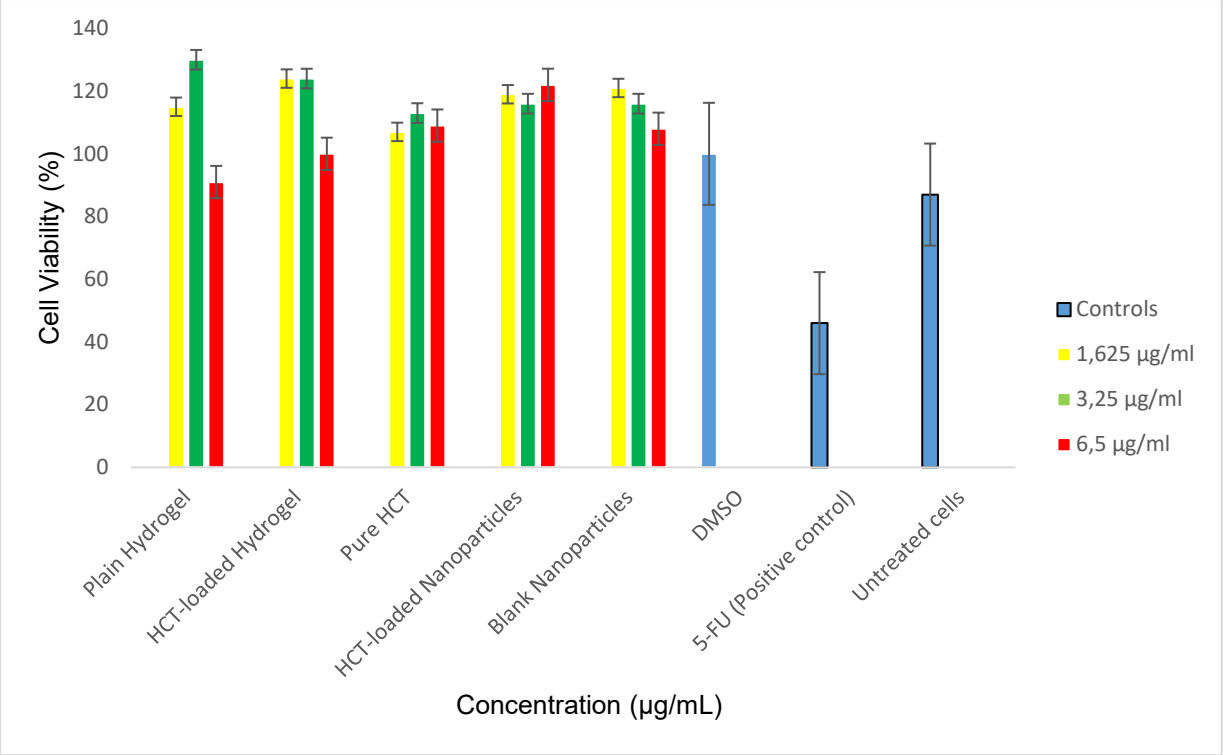
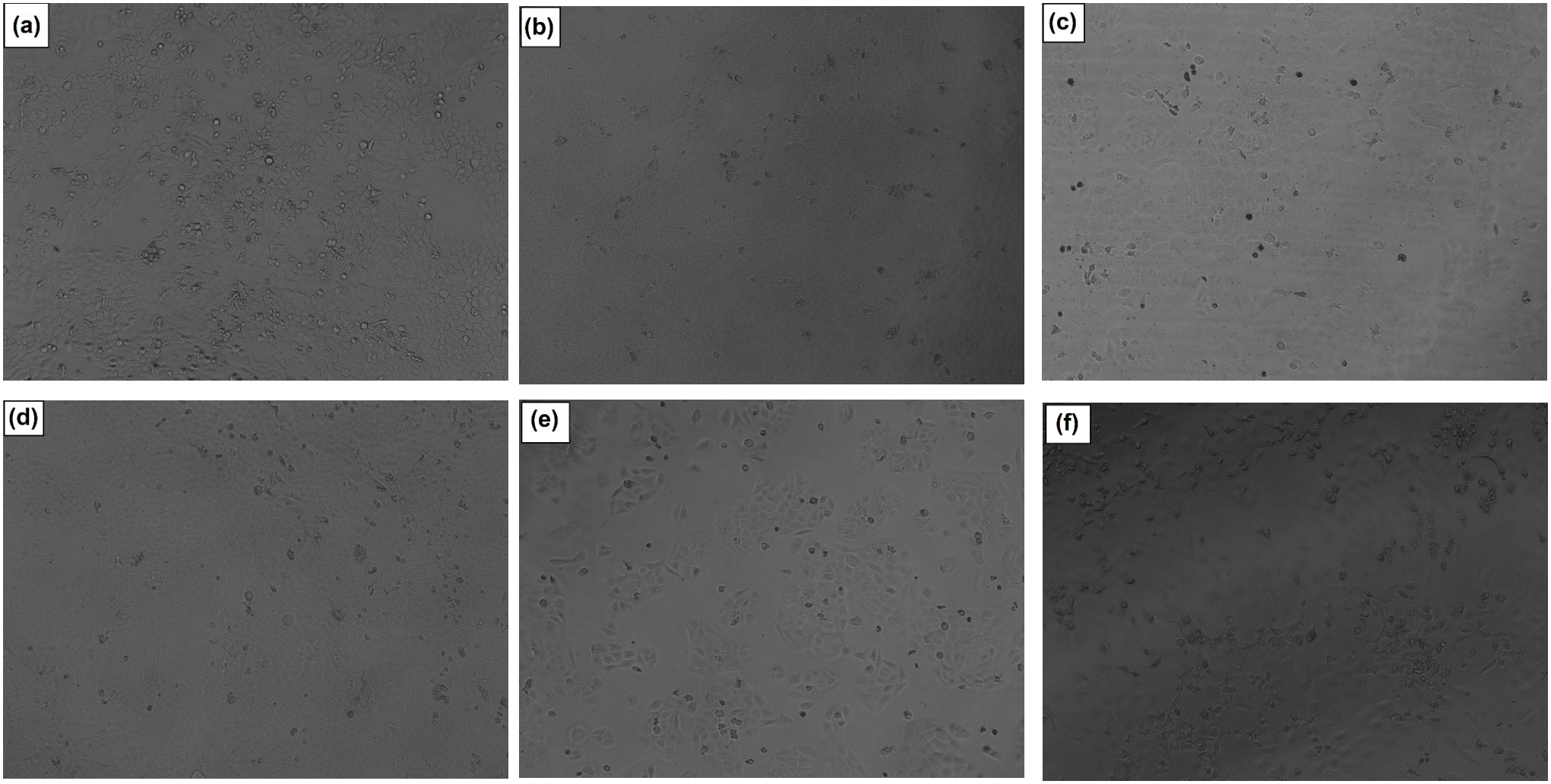


Figure 3.12 HaCaT Cell Viability (%) following treatment after 48 hours. The graph shows cell viability following MTT Assay of the treated cells against the controls.

A dose-response relationship is observed with respect to the Plain hydrogel and Blank nanoparticles – the higher the concentration, the lower the cell viability. However, this is reversed for the HCT-loaded nanoparticles, where the concentration of the drug is directly proportional to the cell viability. The ability for the treated cells to maintain viability alludes to the biocompatibility of the polymers used in the synthesis of the nanoparticles as well as the hydrogel carrier. Furthermore, it demonstrates the applicability of the thermo-responsive hydrogel in the treatment of inflammatory skin conditions.

Microscopic analysis demonstrated internalization of the HCT-loaded nanoparticles, Blank nanoparticles, Pure HCT, HCT-loaded hydrogel, Plain hydrogel, and the Controls (5-FU, DMSO, and Untreated cells:


(a)
(b)
(c)
(d)
(e)
(f)

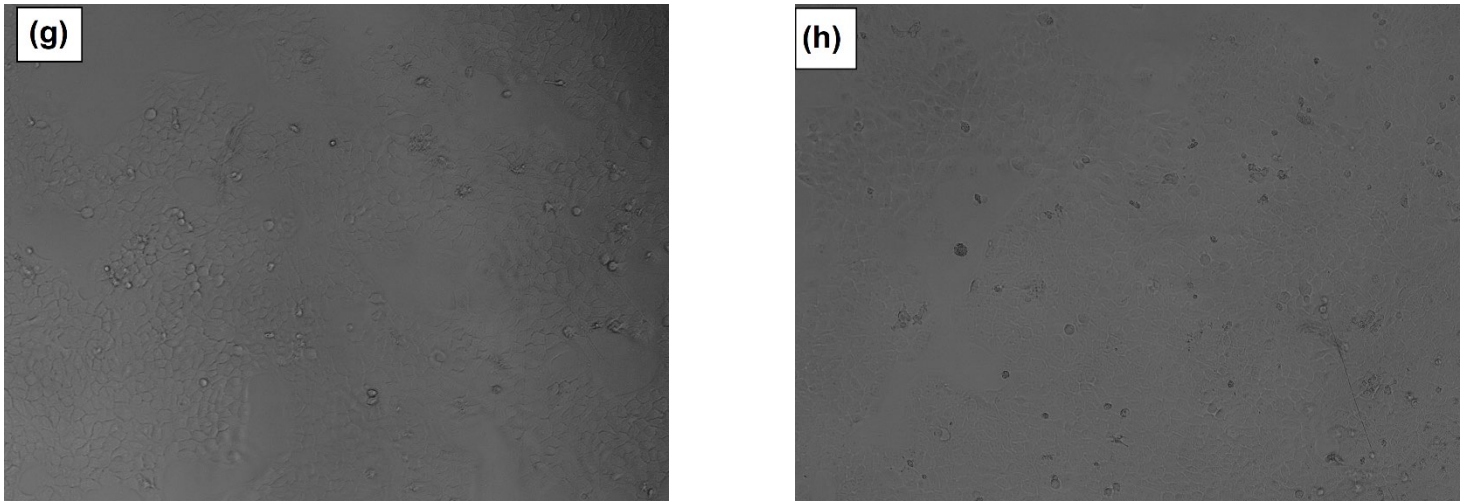


Figure 3.13 Light microscopy images of the (a) Plain Hydrogel, (b) HCT-Loaded hydrogel, (c) Pure HCT, (d) HCT-loaded nanoparticles, (e) Blank nanoparticles, (f) 5-FU, (g) Untreated cells, and (h) DMSO control after 48 hours treatment.

CHAPTER 4. CONCLUSION AND FUTURE RECOMMENDATIONS

PV is a chronic, incurable, inflammatory skin condition with a severe impact on the quality of life. In this present study, a thermo-responsive polymeric hydrogel system loaded with anti-psoriasis drug was synthesized. Nanoparticles with a diameter of 110.5 nm, zeta potential -58,7 mV, and PdI of 0.15 were successfully synthesised and loaded with HCT (DEE = 76%). SEM analysis confirmed the spherical shape of the NLCs. UV/Vis spectroscopy (λ = 245 nm) confirmed the linear correlation between the concentration of the drug and absorbance. Physicochemical characterizations of the NLCs (drug-loaded and non-drug loaded), as well as of the pure HCT drug, were performed using DSC, FTIR, and TGA – these confirmed the presence of HCT within the nanoparticle structures. A thermo-responsive hydrogel with SGTT ~ 35 ºC was successfully synthesized. Drug release profiles for HCT were controlled by pH of the release medium. The release of HCT was slower and more sustained from the CMC thermo-responsive hydrogel in comparison to free nanoparticles. *In vitro* cytotoxicity results showed that the synthesized HCT-loaded, thermo-responsive hydrogel system is safe and tolerable for application to the skin due to the high cell viability demonstrated by both the HCT-loaded nanoparticles as well as the HCT-loaded hydrogel. Microscopic studies show internalization of the hydrogel system showing biocompatibility and sustained release of the system.

Further studies with *in vivo* models should be conducted to assess this as a potential novel therapeutic outlet for the treatment of inflammatory skin diseases.

CHAPTER 5. REFERENCES

Abbas, N., Arshad, M.S., Hussain, A., Irfan, M., Ahsan, M., Rasool, M.F. and ur Rehman, M.H., 2017. Development and validation of a spectroscopic method for the simultaneous analysis of miconazole nitrate and hydrocortisone acetate in pharmaceutical dosage form. *Tropical Journal of Pharmaceutical Research*, *16*(2), pp.413-420.

Abdulghani, M., Al Sheik, A., Alkhawajah, M., Ammoury, A., Behrens, F., Benchikhi, H., Benkaidali, I., Doss, N., Gendy, A.E., Mokhtar, I. and Odendaal, D., (2011). Management of psoriasis in Africa and the Middle East: a review of current opinion, practice and opportunities for improvement. *Journal of International Medical Research*, 39(5), pp.1573-1588.

Afonina, I.S., Van Nuffel, E. and Beyaert, R., 2021. Immune responses and therapeutic options in psoriasis. *Cellular and Molecular Life Sciences*, pp.1-19.

Al Raddadi, A.A., Fatani, M.I., Shaikh, Y.H., Thaci, D., Al Reshaid, A.A., Al-Eisa, A.M., Alghamdi, W.A., Abdulfattah, H.Y., Al Belbisi, Z.M., Atawi, A.C. and Alajroush, W.A., 2011. Adopted guidelines of care for the topical management of psoriasis from American and German guidelines. *Journal of the Saudi Society of Dermatology & Dermatologic Surgery*, *15*(1), pp.5-13.

Alahmadi, H.A., Alsulaiti, R., Abdulla, J. and BAO, M., 2020. Topical Steroids Induced Adrenal Insufficiency. *Bahrain Medical Bulletin*, *42*(3).

Alexander, A., Dwivedi, S., Giri, T.K., Saraf, S., Saraf, S. and Tripathi, D.K., 2012. Approaches for breaking the barriers of drug permeation through transdermal drug delivery. *Journal of Controlled Release*, *164*(1), pp.26-40.

Algahtani, M.S., Ahmad, M.Z. and Ahmad, J., 2020. Nanoemulsion loaded polymeric hydrogel for topical delivery of curcumin in psoriasis. *Journal of Drug Delivery Science and Technology*, *59*, p.101847.

Ali, H.S., York, P. and Blagden, N., 2009. Preparation of hydrocortisone nanosuspension through a bottom-up nanoprecipitation technique using microfluidic reactors. *International journal of pharmaceutics*, *375*(1-2), pp.107-113.

Ali, M.F.M., Salah, M., Rafea, M. and Saleh, N., 2008. Liposomal methotrexate hydrogel for treatment of localized psoriasis: preparation, characterization and laser targeting. *Medical Science Monitor*, *14*(12), pp.PI66-PI74.

Altamimi, M.A., Elzayat, E.M., Qamar, W., Alshehri, S.M., Sherif, A.Y., Haq, N. and Shakeel, F. (2019). Evaluation of the bioavailability of hydrocortisone when prepared as solid dispersion. *Saudi Pharmaceutical Journal*, *27*(5), pp.629-636.

Altomare, L., Bonetti, L., Campiglio, C.E., De Nardo, L., Draghi, L., Tana, F. and Farè, S., 2018. Biopolymer-based strategies in the design of smart medical devices and artificial organs. *The International journal of artificial organs*, *41*(6), pp.337-359.

Andonova, V.Y., Peneva, P.T., Apostolova, E.G., Dimcheva, T.D., Peychev, Z.L. and Kassarova, M.I. 2017 Carbopol hydrogel/sorbitan monostearate-almond oil based organogel biphasic formulations: Preparation and characterization of the bigels. *Tropical Journal of Pharmaceutical Research*, *16*(7), pp.1455-1463.

Armstrong, A.W. and Read, C., 2020. Pathophysiology, clinical presentation, and treatment of psoriasis: a review. *Jama*, *323*(19), pp.1945-1960.

Atanasova, D., Staneva, D. and Grabchev, I., 2021. Textile Materials Modified with Stimuli-Responsive Drug Carrier for Skin Topical and Transdermal Delivery. Materials 2021, 14, 930.

Avasatthi, V., Pawar, H., Dora, C.P., Bansod, P., Gill, M.S. and Suresh, S. 2016. A novel hydrogel formulation of methotrexate for topical treatment of psoriasis: optimization, in vitro and in vivo evaluation. *Pharmaceutical development and technology*, *21*(5), pp.554-562.

Awasthi, G.P., Kaliannagounder, V.K., Park, J., Maharjan, B., Shin, M., Yu, C., Park, C.H. and Kim, C.S., 2021. Assembly of porous graphitic carbon nitride nanosheets into electrospun polycaprolactone nanofibers for bone tissue engineering. *Colloids and Surfaces A: Physicochemical and Engineering Aspects*, p.126584.

Baliwag, J., Barnes, D.H. and Johnston, A. 2015 Cytokines in psoriasis. *Cytokine*, 73(2), pp.342-350.

Barrera-Rivera, K.A. and Martínez-Richa, A. 2018 L-Lysine-Modified Poly (ester-urethane) Based on Polycaprolactone for Controlled Release of Hydrocortisone. In *Green Polymer Chemistry: New Products, Processes, and Applications* (pp. 163-175). American Chemical Society.

Belinchón, I., Rivera, R., Blanch, C., Comellas, M. and Lizán, L., 2016. Adherence, satisfaction and preferences for treatment in patients with psoriasis in the European Union: a systematic review of the literature. *Patient preference and adherence, 10*, p.2357.

Bender, E.A., Adorne, M.D., Colomé, L.M., Abdalla, D.S., Guterres, S.S. and Pohlmann, A.R., 2012. Hemocompatibility of poly (ε-caprolactone) lipid-core nanocapsules stabilized with polysorbate 80-lecithin and uncoated or coated with chitosan. *International journal of pharmaceutics*, *426*(1-2), pp.271-279.

Bessar, H., Venditti, I., Benassi, L., Vaschieri, C., Azzoni, P., Pellacani, G., Magnoni, C., Botti, E., Casagrande, V., Federici, M. and Costanzo, A. 2016. Functionalized gold nanoparticles for topical delivery of methotrexate for the possible treatment of psoriasis. *Colloids and Surfaces B: Biointerfaces*, *141*, pp.141-147.

Bigliardi, P.L. 2018. Role of skin pH in psoriasis. *pH of the Skin: Issues and Challenges*, *54*, pp.108-114.

Budamakuntla, L., Loganathan, E., Gundappa, P. and Sreelakshmi, K.T., 2017. IL 17 cytokine in psoriasis: before and after methotrexate and NBUVB phototherapy: a longitudinal study. *Clin Dermatol Res J* 2, 1, p.2.

Caló, E. and Khutoryanskiy, V.V., 2015. Biomedical applications of hydrogels: A review of patents and commercial products. *European Polymer Journal*, *65*, pp.252-267.

Caso, F., Chimenti, M.S., Navarini, L., Ruscitti, P., Peluso, R., Girolimetto, N., Del Puente, A., Giacomelli, R., Scarpa, R. and Costa, L., 2020. Metabolic Syndrome and psoriatic arthritis: considerations for the clinician. *Expert review of clinical immunology*, *16*(4), pp.409-420.

Cavalli, R., Peira, E., Caputo, O. and Gasco, M.R., 1999. Solid lipid nanoparticles as carriers of hydrocortisone and progesterone complexes with β-cyclodextrins. *International journal of pharmaceutics*, *182*(1), pp.59-69.

Chatterjee, S., Hui, P. C. L. and Kan, C. wai 2018'Thermoresponsive hydrogels and their biomedical applications: Special insight into their applications in textile based transdermal therapy', *Polymers*, 10(5). doi: 10.3390/polym10050480.

Chen, H., Sun, J., Yang, H., Sun, Q., Zhang, J., Gu, J., Wen, H., Li, M., Liu, X., Yang, H. and Lou, D., 2020. Fixed combination of tazarotene and betamethasone dipropionate for treatment of psoriasis vulgaris: The result of a phase 3, multicenter, randomized controlled trial. *The Journal of dermatology*, *47*(7), pp.728-734.

Chen, P., Xie, F., Tang, F. and McNally, T., 2020. Structure and properties of thermomechanically processed chitosan/carboxymethyl cellulose/graphene oxide polyelectrolyte complexed bionanocomposites. *International journal of biological macromolecules*, *158*, pp.420-429.Sharadha, M., Gowda, D., Gupta, N., *et al.* 2020 'An overview on topical drug delivery system – updated review', *International Journal of Research in Pharmaceutical Sciences*, 11(1), pp. 368–385. doi: 10.26452/ijrps.v11i1.1831.

Cheng, Y.H., Ko, Y.C., Chang, Y.F., Huang, S.H. and Liu, C.J.L., 2019. Thermosensitive chitosan-gelatin-based hydrogel containing curcumin-loaded nanoparticles and latanoprost as a dual-drug delivery system for glaucoma treatment. *Experimental Eye Research*, *179*, pp.179-187.

Ciolacu, D.E., Nicu, R. and Ciolacu, F., 2020. Cellulose-Based Hydrogels as Sustained Drug-Delivery Systems. *Materials*, *13*(22), p.5270. Schön, M.P. and Erpenbeck, L., 2018. The interleukin-23/interleukin-17 axis links adaptive and innate immunity in psoriasis. *Frontiers in immunology*, 9, p.1323.

Colombo, I., Sangiovanni, E., Maggio, R., Mattozzi, C., Zava, S., Corbett, Y., Fumagalli, M., Carlino, C., Corsetto, P.A., Scaccabarozzi, D. and Calvieri, S. 2017. HaCaT cells as a reliable in vitro differentiation model to dissect the inflammatory/repair response of human keratinocytes. *Mediators of inflammation*, *2017*.

Croisfelt, F.M., Tundisi, L.L., Ataide, J.A., Silveira, E., Tambourgi, E.B., Jozala, A.F., Souto, E.M.B. and Mazzola, P.G., 2019. Modified-release topical hydrogels: a ten-year review. *Journal of materials science*, pp.1-21.

Da Silva, A.L.M., Contri, R.V., Jornada, D.S., Pohlmann, A.R. and Guterres, S.S., 2013. Vitamin K1–loaded lipid-core nanocapsules: physicochemical characterization and in vitro skin permeation. *Skin Research and Technology*, *19*(1), pp.e223-e230.

Danaei, M., Dehghankhold, M., Ataei, S., Hasanzadeh Davarani, F., Javanmard, R., Dokhani, A., Khorasani, S. and Mozafari, M.R. 2018. Impact of particle size and polydispersity index on the clinical applications of lipidic nanocarrier systems. *Pharmaceutics*, *10*(2), p.57.

Dattola, A., Silvestri, M., Bennardo, L., Passante, M., Rizzuto, F., Dastoli, S., Patruno, C., Bianchi, L. and Nisticò, S.P., 2020. A novel vehicle for the treatment of psoriasis. *Dermatologic therapy*, *33*(1), p.e13185.

de Oliveira, É.L., Ferreira, S.B., de Castro-Hoshino, L.V., Campanholi, K.D.S., Calori, I.R., de Morais, F.A., Kimura, E., da Silva Junior, R.C., Bruschi, M.L., Sato, F. and Hioka, N., 2021. Thermoresponsive Hydrogel-Loading Aluminum Chloride Phthalocyanine as a Drug Release Platform for Topical Administration in Photodynamic Therapy. *Langmuir*.

Dehkharghani, R.A., Hosseinzadeh, M., Nezafatdoost, F. and Jahangiri, J., 2018. Application of methodological analysis for hydrocortisone nanocapsulation in biodegradable polyester and MTT assay. *Polymer Science, Series A*, *60*(6), pp.770-776.

Dehshahri, A., Kumar, A., Madamsetty, V.S., Uzieliene, I., Tavakol, S., Azedi, F., Fekri, H.S., Zarrabi, A., Mohammadinejad, R. and Thakur, V.K., 2021. New Horizons in Hydrogels for Methotrexate Delivery. *Gels*, *7*(1), p.2.

Del Rosso, J.Q., 2020. Topical corticosteroid therapy for psoriasis—a review of clobetasol propionate 0.025% cream and the clinical relevance of penetration modification. *The Journal of clinical and aesthetic dermatology*, *13*(2), p.22.

Dhawan, S.S., Blyumin, M.L., Pearce, D.J. and Feldman, S.R., 2005. Tazarotene cream (0.1%) in combination with betamethasone valerate foam (0.12%) for plaque-type psoriasis. *Journal of drugs in dermatology: JDD*, *4*(2), pp.228-230.

Don, T.M., Huang, M.L., Chiu, A.C., Kuo, K.H., Chiu, W.Y. and Chiu, L.H., 2008. Preparation of thermo-responsive acrylic hydrogels useful for the application in transdermal drug delivery systems. *Materials Chemistry and Physics*, *107*(2-3), pp.266-273.

Drugbank, 2021 *Dexamethasone* [Onlime]. Available at: <https://go.drugbank.com/drugs/DB01234>. [Accessed on 24 Mar 2021]

Drugs.com. 2021. *Hydrocortisone topical Uses, Side Effects & Warnings - Drugs.com*. [online] Available at: <https://www.drugs.com/mtm/hydrocortisone-topical.htmL> [Accessed 13 February 2021].

El-sayed, S., Mahmoud, K., Fatah, A., and Hassen, A. 2011 'DSC , TGA and dielectric properties of carboxymethyl cellulose / polyvinyl alcohol blends', *Physica B: Physics of Condensed Matter*. Elsevier, 406(21), pp. 4068–4076. doi: 10.1016/j.physb.2011.07.050.

Elzein, T., Nasser-Eddine, M., Delaite, C., Bistac, S. and Dumas, P., 2004. FTIR study of polycaprolactone chain organization at interfaces. *Journal of colloid and interface science*, *273*(2), pp.381-387.

Engler D., Chezuba H.P., Masuku, P. 2017 'Psoriasis', *South African Pharmacy Journal*, 84(5), pp. 38–42. doi: 10.1017/CBO9781107415324.004.

Fatehi, P., Baba, A.S. and Misran, M., 2020. Preparation and characterization of palm oil in water microemulsion for application in the food industry. *British Food Journal*.

Ghate, V. M., Kodoth, A., Shah, A., *et al.* 2019 'Colloidal nanostructured lipid carriers of pentoxifylline produced by microwave irradiation ameliorates imiquimod-induced psoriasis in mice', *Colloids and Surfaces B: Biointerfaces*. Elsevier, 181(March), pp. 389–399. doi: 10.1016/j.colsurfb.2019.05.074.

Gill, P., Moghadam, T., and Ranjbar, B. 2014 'Differential Scanning Calorimetry Techniques : Applications in Biology and Differential Scanning Calorimetry

Techniques : Applications in Biology and Nanoscience', *Journal of Biomolecular Techniques*, 21(4), pp. 167–193.

Giri, T. K. 2019 'Solid lipid nanoparticles for the delivery of drug molecules', in Grumezescu, V.; Grumezescu, A. (ed.) *Materials for Biomedical Engineering: Organic Micro and Nanostructures*. 1st edn. Elsevier Inc., pp. 551–576. doi: 10.1016/B978-0-12-818433-2.00016-9.

Gold, L.S., Bhatia, N., Tallman, A.M. and Rubenstein, D.S., 2021. A phase 2b, randomized clinical trial of tapinarof cream for the treatment of plaque psoriasis: Secondary efficacy and patient-reported outcomes. *Journal of the American Academy of Dermatology*, *84*(3), pp.624-631.

Gold, L.S., Lebwohl, M., Menter, A., Villumsen, J., Rosen, M. and Koo, J., 2016. Aerosol foam formulation of fixed combination calcipotriene plus betamethasone dipropionate is highly efficacious in patients with psoriasis vulgaris: pooled data from three randomized controlled studies. *Journal of drugs in dermatology: JDD*, *15*(8), pp.951-957.

Gradzielski, M., Duvail, M., de Molina, P.M., Simon, M., Talmon, Y. and Zemb, T., 2021. Using Microemulsions: Formulation Based on Knowledge of Their Mesostructure. *Chemical Reviews*.

Graham, S., Marina, P. F. and Blencowe, A. 2019 'Thermoresponsive polysaccharides and their thermoreversible physical hydrogel networks', *Carbohydrate Polymers*. Elsevier Ltd., 207, pp. 143–159. doi: 10.1016/j.carbpol.2018.11.053.

Greive, K. A. and Barnes, T. M. 2016 'Bioequivalence of 0.1% mometasone furoate lotion to 0.1% mometasone furoate hydrogel', *Australasian Journal of Dermatology*, 57(2), pp. e39–e45. doi: 10.1111/ajd.12275.

Grozdev, I. and Korman, N.J., 2021. Psoriasis: epidemiology, potential triggers, disease course. In *Advances in psoriasis* (pp. 27-37). Springer, Cham.

Güngör, S., Kahraman, E. and Özsoy, Y., 2015. Polymeric micelles for cutaneous drug delivery. *Nano Based Drug Delivery. Naik J (Ed.). IAPC Publishing, Zagreb, Croatia*, pp.369-384.

Gyles, D., Castro, L., Silva, J., *et al.* 2017 'A review of the designs and prominent biomedical advances of natural and synthetic hydrogel formulations', *European Polymer Journal*, 88, pp. 373–392. doi: 10.1016/j.eurpolymj.2017.01.027.

Haidari, W., Glines, K.R., Cline, A. and Feldman, S.R., 2020. Adherence in Acne. In *Treatment Adherence in Dermatology* (pp. 85-97). Springer, Cham. Thakur, V.; Thakur, M.; and Voicu, S. (ed.) 2018 *Polymer Gels: Perspectives and Applications*. Singapore: Springer Nature. doi: 10.1007/978-981-10-6080-9_5.

Hoffman, A. S. 2013 'Stimuli-responsive polymers : Biomedical applications and challenges for clinical translation ☆', *Advanced Drug Delivery Reviews*. Elsevier B.V., 65(1), pp. 10–16. doi: 10.1016/j.addr.2012.11.004.

Hsu, D.Y. and Gniadecki, R., 2016. Patient adherence to biologic agents in psoriasis. *Dermatology, 232*(3), pp.326-333.

Huang, H. Qi, X., Chen, Y., and Wu, Z. 2019 'Thermo-sensitive hydrogels for delivering biotherapeutic molecules: A review', *Saudi Pharmaceutical Journal*. King Saud University, 27(7), pp. 990–999. doi: 10.1016/j.jsps.2019.08.001.

Huang, H., Liu, J., Liu, H., Evrendilek, F. and Buyukada, M., 2020. Pyrolysis of water hyacinth biomass parts: Bioenergy, gas emissions, and by-products using TG-FTIR and Py-GC/MS analyses. *Energy Conversion and Management*, *207*, p.112552.

Huang, T.H., Lin, C.F., Alalaiwe, A., Yang, S.C. and Fang, J.Y., 2019. Apoptotic or antiproliferative activity of natural products against keratinocytes for the treatment of psoriasis. *International journal of molecular sciences*, *20*(10), p.2558.

Iskandar, I.Y.K., Parisi, R., Griffiths, C.E.M., Ashcroft, D.M. and Global Psoriasis Atlas, 2021. Systematic review examining changes over time and variation in the incidence and prevalence of psoriasis by age and gender. *British Journal of Dermatology*, *184*(2), pp.243-258.

Kahraman, E., Aydilek, N. and Güngör, S., 2020. Recent Approaches on Novel Topical Delivery Systems for Atopic Dermatitis Treatment. *Recent Patents on Drug Delivery & Formulation*, *14*(3), pp.191-200.

Kang, L., Yap, C.W., Lim, P.F.C., Chen, Y.Z., Ho, P.C., Chan, Y.W., Wong, G.P. and Chan, S.Y. 2007. Formulation development of transdermal dosage forms: Quantitative

structure-activity relationship model for predicting activities of terpenes that enhance drug penetration through human skin. *Journal of Controlled Release*, *120*(3), pp.211-219.

Katas, H., Hussain, Z. and Ling, T.C., 2012. Chitosan nanoparticles as a percutaneous drug delivery system for hydrocortisone. *Journal of Nanomaterials*, *2012*.

Kaur, N., Sharma, K. and Bedi, N., 2018. Topical nanostructured lipid carrier based hydrogel of mometasone furoate for the treatment of psoriasis. *Pharmaceutical nanotechnology*, *6*(2), pp.133-143.

Khurana, S., Jain, N.K. and Bedi, P.M.S. 2013. Nanoemulsion based gel for transdermal delivery of meloxicam: physico-chemical, mechanistic investigation. *Life sciences*, *92*(6-7), pp.383-392.

Kim, E.S. and Frampton, J.E., 2016. Calcipotriol/betamethasone dipropionate foam: a review in plaque psoriasis. *Drugs*, *76*(15), pp.1485-1492.

Kim, Y. and Matsunaga, Y. T. 2017 'Thermo-responsive polymers and their application', *Journal of Materials Chemistry B*. Royal Society of Chemistry, 5, pp. 4307–4321. doi: 10.1039/C7TB00157F.

Kleyn, E.C., Morsman, E., Griffin, L., Wu, J.J., Cm van de Kerkhof, P., Gulliver, W., van der Walt, J.M. and Iversen, L., 2019. Review of international psoriasis guidelines for the treatment of psoriasis: recommendations for topical corticosteroid treatments.

Klouda, L. 2015 'Thermoresponsive hydrogels in biomedical applications A seven-year update', *European Journal of Pharmaceutics and Biopharmaceutics*. Elsevier B.V., 97, pp. 338–349. doi: 10.1016/j.ejpb.2015.05.017.

Kumar, P., Nagarajan, A. and Uchil, P.D. 2018. Analysis of cell viability by the MTT assay. *Cold Spring Harbor Protocols*, *2018*(6), pp.pdb-prot095505.

Kumar, R., Ayyanar, S., Jayaraj, P., Sivaramakrishna, A., Rajagopalan, S., Parthasarathy, S. and Desikan, R., 2021. Hydrogel Formulation as Efficient Drug Carrier and Delivery for Selected Skin Diseases. In *Nano Hydrogels* (pp. 181-203). Springer, Singapore.

Kumar, S., Prasad, M. and Rao, R., 2021. Topical delivery of clobetasol propionate loaded nanosponge hydrogel for effective treatment of psoriasis: Formulation,

physicochemical characterization, antipsoriatic potential and biochemical estimation. *Materials Science and Engineering: C*, *119*, p.111605.

Lale, S.V. and Koul, V., 2018. Stimuli-Responsive Polymeric Nanoparticles for Cancer Therapy. In *Polymer Gels* (pp. 27-54). Springer, Singapore.

Lanzalaco, S. and Armelin, E., 2017. Poly (n-isopropylacrylamide) and copolymers: A review on recent progresses in biomedical applications. *Gels*, *3*(4), p.36.

Lee, C.M., Lim, S., Kim, G.Y., Kim, D.W., Rhee, J.H. and Lee, K.Y., 2005. Rosin nanoparticles as a drug delivery carrier for the controlled release of hydrocortisone. *Biotechnology letters*, *27*(19), pp.1487-1490.

Li, L., He, Y., Zheng, X., Yi, L. and Nian, W., 2021. Progress on Preparation of pH/Temperature-Sensitive Intelligent Hydrogels and Applications in Target Transport and Controlled Release of Drugs. *International Journal of Polymer Science*, *2021*. Tipa, C., Cidade, M.T., Vieira, T., Silva, J.C., Soares, P.I. and Borges, J.P., 2021. A New Long-Term Composite Drug Delivery System Based on Thermo-Responsive Hydrogel and Nanoclay. *Nanomaterials*, *11*(1), p.25.Rendon, A. and Schäkel, K. 2019. Psoriasis pathogenesis and treatment. *International journal of molecular sciences*, 20(6), p.1475.

Li, X., Yang, Q., Zheng, J., Gu, H., Chen, K., Jin, H., He, C., Xu, A.E., Xu, J., Zhang, J. and Yu, W., 2020. Efficacy and safety of a topical moisturizer containing linoleic acid and ceramide for mild-to-moderate psoriasis vulgaris: A multicenter randomized controlled trial. *Dermatologic Therapy*, *33*(6), p.e14263.

Limón, D., Dominguez, K., Ramirez, M., *et al.* 2019 'Nanostructured supramolecular hydrogels: Towards the topical treatment of Psoriasis and other skin diseases', *Colloids and Surfaces B: Biointerfaces*. Elsevier, 181(March), pp. 657–670. doi: 10.1016/j.colsurfb.2019.06.018.

Lyseng-Williamson, K. A. 2016 'Mometasone furoate 0.1 % ointment and hydrogel: a guide to their use in corticosteroid-responsive dermatoses', *Drugs and Therapy Perspectives*. Springer International Publishing, 32(10), pp. 407–413. doi: 10.1007/s40267-016-0339-9.

Mahmoudi, M., Saeidian, H., Mirjafary, Z. and Mokhtari, J. 2020. Preparation and characterization of memantine loaded polycaprolactone nanocapsules for Alzheimer's disease. *Journal of Porous Materials*, pp.1-8.

Mao, K.L., Fan, Z.L., Yuan, J.D., Chen, P.P., Yang, J.J., Xu, J., ZhuGe, D.L., Jin, B.H., Zhu, Q.Y., Shen, B.X. and Sohawon, Y., 2017. Skin-penetrating polymeric nanoparticles incorporated in silk fibroin hydrogel for topical delivery of curcumin to improve its therapeutic effect on psoriasis mouse model. *Colloids and Surfaces B: Biointerfaces*, *160*, pp.704-714.

Maqbool, S., Ihtesham, A., Langove, M.N., Jamal, S., Jamal, T. and Safian, H.A., 2021. Neuro-dermatological association between psoriasis and depression: an immune-mediated inflammatory process validating skin-brain axis theory. *AIMS Neuroscience*, *8*(3), pp.340-354.

Marieb, E. N. and Hoehn, K. 2012 *Human Anatomy & Physiology*. 9th edn. Boston: Pearson.

Mehrmal, S., Uppal, P., Nedley, N., Giesey, R.L. and Delost, G.R., 2021. The global, regional, and national burden of psoriasis in 195 countries and territories, 1990 to 2017: a systematic analysis from the Global Burden of Disease Study 2017. *Journal of the American Academy of Dermatology*, *84*(1), pp.46-52.

Mendelson-Mastey, C., Larush, L., Danino, D. and Magdassi, S. 2017. Synthesis of magnesium chloride nanoparticles by the water/oil nanoemulsion evaporation. *Colloids and Surfaces A: Physicochemical and Engineering Aspects*, *529*, pp.930-935.

Meng, S., Sun, L., Wang, L., *et al.* 2019 'Loading of water-insoluble celastrol into niosome hydrogels for improved topical permeation and anti-psoriasis activity', *Colloids and Surfaces B: Biointerfaces*. Elsevier, 182(July), p. 110352. doi: 10.1016/j.colsurfb.2019.110352.

Menter, M. A. and Ryan, C. (ed.) 2017 *Psoriasis*. 2nd edn. Boca Raton: CRC Press.

Merck 2013 'ELOCON (Mometasone Furoate) Lable'. MERCK, pp. 1–7.

Mohamed, M., Jafar, J., Ismail, A., *et al.* 2017 'Fourier Transform Infrared (FTIR) Spectroscopy', in *Membrane Characterization*. 1st edn. Elsevier B.V., pp. 3–29. doi: 10.1016/B978-0-444-63776-5.00001-2.

Morankar, P.G., Kumbhare, M.R., Shelke, S.J. and Diwane, C.M., 2021. Enhancement of Skin Permeability and Anti-Inflammatory, Antipsoriatic Efficacy of Curcumin through a Gel Formulation. *Innoriginal: International Journal of Sciences*, pp.22-29.

Nandiyanto, A.B.D., Oktiani, R. and Ragadhita, R., 2019. How to read and interpret FTIR spectroscope of organic material. *Indonesian Journal of Science and Technology*, *4*(1), pp.97-118.

nanoComposix. 2021. *Zeta Potential Measurements*. [online] Available at: <https://nanocomposix.com/pages/zeta-potential-measurements#target> [Accessed 2 February 2021].

Nastiti, C.M., Ponto, T., Abd, E., Grice, J.E., Benson, H.A. and Roberts, M.S., 2017. Topical nano and microemulsions for skin delivery. *Pharmaceutics*, *9*(4), p.37.

Ni, X. and Lai, Y., 2020. Keratinocyte: A trigger or an executor of psoriasis?. *Journal of leukocyte biology*, *108*(2), pp.485-491.

Nita, L., Chiriac, A., Rusu, A., *et al.* 2020 'Stimuli Responsive Scaffolds Based on Carboxymethyl Starch and Poly(2-Dimethylaminoethyl Methacrylate) for Anti-Inflammatory Drug Delivery.', *Macromolecular bioscience*, 1900412, p. e1900412. doi: 10.1002/mabi.201900412.

OpenStax College 2015 'Chapter 5: The Integumentary System' in Anatomy Physiology. Houston: OpenStax College. doi: 10.1177/089686081503501s03

Palmer, B.C. and DeLouise, L.A., 2016. Nanoparticle-enabled transdermal drug delivery systems for enhanced dose control and tissue targeting. *Molecules*, *21*(12), p.1719.

Pannu, S. and Rosmarin, D., 2021. Psoriasis in Patients with Metabolic Syndrome or Type 2 Diabetes Mellitus: Treatment Challenges. *American Journal of Clinical Dermatology*, pp.1-8.

Panonnummal, R., Jayakumar, R. and Sabitha, M. 2017 'Comparative anti-psoriatic efficacy studies of clobetasol loaded chitin nanogel and marketed cream', *European Journal of Pharmaceutical Sciences*. Elsevier B.V., 96, pp. 193–206. doi: 10.1016/j.ejps.2016.09.007.

Pantshwa, J., Choonara, Y.E., Kumar, P., du Toit, L.C., Penny, C., and Pillay, V., 2017. Synthesis of novel amphiphilic poly (N-isopropylacrylamide)-b-poly (aspartic acid) nanomicelles for potential targeted chemotherapy in ovarian cancer. *Journal of Drug Delivery Science and Technology*, *39*, pp.308-323.

Rapalli, V.K., Waghule, T., Gorantla, S., Dubey, S.K., Saha, R.N. and Singhvi, G., 2020. Psoriasis: pathological mechanisms, current pharmacological therapies, and emerging drug delivery systems. *Drug Discovery Today*. Spada, F., Barnes, T. M. and Greive, K. A. 2018 'Comparative safety and efficacy of topical mometasone furoate with other topical corticosteroids', *Australasian Journal of Dermatology*, 59(3), pp. e168–e174. doi: 10.1111/ajd.12762

Richards, H.L., Fortune, D.G. and Griffiths, C.E.M., 2006. Adherence to treatment in patients with psoriasis. *Journal of the European Academy of Dermatology and Venereology*, *20*(4), pp.370-379.

Rimmer, S. 2011 Biomedical hydrogels: Biochemistry, manufacture and medical applications. 1st edn, *Biomedical Hydrogels: Biochemistry, Manufacture and Medical Applications*. 1st edn. Edited by Steve Rimmer. Cambridge: Woodhead Publishing. doi: 10.1533/9780857091383.

Rocha, A.C., Bortoletto, M.C., da Costa, A.C., Oyafuso, L.K., Sanudo, A. and Tomita, L.Y., 2021. Low serum lycopene, and adequate α-tocopherol levels in patients with psoriasis: A cross-sectional study. *Nutrition and Health*, p.02601060211014127.

Rodríguez-Rodríguez, R., Espinosa-Andrews, H., Velasquillo-Martínez, C. and García-Carvajal, Z.Y., 2020. Composite hydrogels based on gelatin, chitosan and polyvinyl alcohol to biomedical applications: a review. *International Journal of Polymeric Materials and Polymeric Biomaterials*, *69*(1), pp.1-20.

Rosado, C., Silva, C. and Reis, C.P., 2013. Hydrocortisone-loaded poly (ε-caprolactone) nanoparticles for atopic dermatitis treatment. *Pharmaceutical development and technology*, *18*(3), pp.710-718.

Rossiter, D. (ed) 2016 , *South African Medicines Formulary (SAMF)*,12 Edition, Health and Medical Publishing Group, Pretoria

RSC.org. 2020. *Hydrocortisone | The Merck Index Online*. [online] Available at: <https://www.rsc.org/Merck-Index/monograph/m6094/hydrocortisone?q=unauthorize> [Accessed 18 November 2020].

Ruela, A.; Perissinato, A.; Lino, M., Mudrik, P.; and Pereira, G. 2016 'Evaluation of skin absorption of drugs from topical and transdermal formulations', *Brazilian Journal of Pharmaceutical Sciences*, 52(3), pp. 527–544.

Saleem, S., Iqubal, M.K., Garg, S., Ali, J. and Baboota, S., 2020. Trends in nanotechnology-based delivery systems for dermal targeting of drugs: an enticing approach to offset psoriasis. *Expert opinion on drug delivery*, *17*(6), pp.817-838.

Salgado, A., Raposo, S., Marto, J., *et al.* 2014 'Mometasone furoate hydrogel for scalp use: In vitro and in vivo evaluation', *Pharmaceutical Development and Technology*, 19(5), pp. 618–622. doi: 10.3109/10837450.2013.819012.

Segaert, S., Calzavara-Pinton, P., de la Cueva, P., Jalili, A., Lons Danic, D., Pink, A.E., Thaçi, D. and Gooderham, M., 2020. Long-term topical management of psoriasis: the road ahead. *Journal of Dermatological Treatment*, pp.1-10.

Shinde, G., Desai, P., Shelke, S., Patel, R., Bangale, G. and Kulkarni, D. 2020. Mometasone furoate-loaded aspasomal gel for topical treatment of psoriasis: formulation, optimization, in vitro and in vivo performance. *Journal of Dermatological Treatment*, pp.1-12.

Silna, E., Krishnakumar, K., Nair, S., *et al.* 2016 'Hydrogels in Topical Drug Delivery – A Review', *International Journal of Innovative Drug Discovery*, 6(2), pp. 87–93.

Steinhoff, M., Ammoury, A.F., Ahmed, H.M., Gamal, M.F.S. and El Sayed, M.H., 2020. The Unmet Need for Clinical Guidelines on the Management of Patients with Plaque Psoriasis in Africa and the Middle East. *Psoriasis: Targets and Therapy*, *10*, p.23.

Sterry, W.; Sabat, R.; and Phillip, S. (ed.) 2014 *Psoriasis: Diagnosis and Management*. 1st edn. West Sussex: WILEY Blackwell.

Strober, B., van der Walt, J., Armstrong, A., *et al.* 2019 'Clinical Goals and Barriers to Effective Psoriasis Care', *Dermatology and Therapy*. Springer Healthcare, 9(1), pp. 5–18. doi: 10.1007/s13555-018-0279-5.

Suresh, P.K., Singh, P. and Saraf, S., 2013. Novel topical drug carriers as a tool for treatment of psoriasis: progress and advances. *African journal of pharmacy and pharmacology*, *7*(5), pp.138-147.

Svendsen, M.T., Feldman, S.R., Tiedemann, S.N., Sørensen, A.S.S., Rivas, C.M.R. and Andersen, K.E., 2020. Limitations in Health-Care System Resources Affecting Adherence of Patient With Psoriasis to Topical Drugs: A Focus Group Study. *Journal of Psoriasis and Psoriatic Arthritis*, *5*(2), pp.54-60.

Svoboda, S.A., Ghamrawi, R.I., Owusu, D.A. and Feldman, S.R., 2020. Treatment Goals in Psoriasis: Which Outcomes Matter Most?. *American Journal of Clinical Dermatology*, *21*, pp.505-511.

ThermoNicolet 2001 'Introduction to Fourier Transform Infrared Spectrometry'.

Vincent, N., Ramya, D.D. and Vedha, H.B., 2014. Progress in psoriasis therapy via novel drug delivery systems. *Dermatology reports*, *6*(1).

Voss, G.T., Gularte, M.S., de Oliveira, R.L., Luchese, C., Fajardo, A.R. and Wilhelm, E.A. 2020. Biopolymeric films as delivery vehicles for controlled release of hydrocortisone: Promising devices to treat chronic skin diseases. Materials Science and Engineering: C, 114, p.111074.

Wang, Q., Zuo, Z., Kit, C., *et al.* 2019 'Updates on thermosensitive hydrogel for nasal , ocular and cutaneous delivery', *International Journal of Pharmaceutics*. Elsevier, 559(January), pp. 86–101. doi: 10.1016/j.ijpharm.2019.01.030.

Wang, W., Wat, E., Hui, P., et al. 2016 'Dual-functional transdermal drug delivery system with controllable drug loading based on thermosensitive poloxamer hydrogel for atopic dermatitis treatment', Scientific Reports. Nature Publishing Group, 6(December 2015), pp. 1–10. doi: 10.1038/srep24112.

Whalen, K., Finkel, R., and Panavelil, T.(ed.) 2017 *Lippincott Illustrated Reviews: Pharmacology*. 6th edn. Philadelphia: Wolters Kluwer. doi: 10.1201/978131515235.

Witika, B.A. and Walker, R.B., 2021. Preformulation characterization and identification of excipients for nevirapine loaded niosomes. *Die Pharmazie-An International Journal of Pharmaceutical Sciences*, *76*(2-3), pp.77-83.

Wohlrab, J., Neubert, R., Sommer, E., *et al.* 2016 'Ex vivo Cutaneous Bioavailability of Topical Mometasone Furoate in an O/W Preparation', *Skin Pharmacology and Physiology*, 29(5), pp. 273–279. doi: 10.1159/000452743.

Wollina, U., Tirant, M., Vojvodic, A. and Lotti, T., 2019. Treatment of Psoriasis: Novel Approaches to Topical Delivery. *Open access Macedonian journal of medical sciences*, *7*(18), p.3018.

Wong, R., Geyer, S., Weninger, W., *et al.* 2016 'The dynamic anatomy and patterning of skin', *Experimental Dermatology*, 25(2), pp. 92–98. doi: 10.1111/exd.12832.

World Health Organization, 2016. Global report on psoriasis. 2016. *World Health Organization website. http://apps. who. int/iris/bitstream/handle/10665/204417/9789241565189_eng. pdf*.

World Health Organization, 2021. *Non communicable diseases*. [online] Available at: <*https://www.who.int/news-room/fact-sheets/detail/noncommunicable-diseases*> [Accessed 10 May 2021].

Xu, C., Ji, J., Su, T., Su, Z. and Wang, H., 2021. The association of psoriasis and obesity: focusing on IL-17A related immunological mechanisms. *International Journal of Dermatology and Venereology*.

Yang, C. Y. and Kourosh, A. S. 2018 'Inflammatory skin disorders and self-esteem', *International Journal of Women's Dermatology*, 4(1), pp. 23–26. doi: 10.1016/j.ijwd.2017.09.006

Yang, E.J. and Lipner, S.R., 2021. Topical Therapy I: Corticosteroids and Vitamin D Analogues. In *Advances in Psoriasis* (pp. 39-49). Springer, Cham.

Yazdi, M.K., Taghizadeh, A., Taghizadeh, M., Stadler, F.J., Farokhi, M., Mottaghitalab, F., Zarrintaj, P., Ramsey, J.D., Seidi, F., Saeb, M.R. and Mozafari, M., 2020. Agarose-based biomaterials for advanced drug delivery. *Journal of Controlled Release*.

Zoabi, A., Touitou, E. and Margulis, K., 2021. Recent Advances in Nanomaterials for Dermal and Transdermal Applications. *Colloids and Interfaces*, *5*(1), p.18.

Appendix I: Ethical Clearance

UNIVERSITY OF THE WITWATERSRAND, JOHANNESBURG

HUMAN RESEARCH ETHICS COMMITTEE (MEDICAL)

Human Research Ethics Committee (Medical)

Research Office Secretariat:
Faculty of Health Sciences, Phillip Tobias Health Sciences Building, 3rd Floor, Office 301/2/4, 29 Princess of Wales Terrace, Parktown, 2193
Private Bag 3, Wits 2050
Office email: HREC-Medical.ResearchOffice@wits.ac.za
Website: www.wits.ac.za/research/about-our-research/ethics-and-research-integrity/

Ref: W-CBP-210706-01

06/07/2021

TO WHOM IT MAY CONCERN:

Waiver:	This certifies that the following research does not require clearance from the Human Research Ethics Committee (Medical)
Investigator:	Mr Matsoso Mohlomi
Supervisor:	Prof Pierre Kondiah
Department:	Pharmacy and Pharmacology
Project title:	Design of a topical anti-psoriatic hydrogel drug delivery system for the treatment of psoriasis vulgaris
Reason:	*In vitro* laboratory study using cell lines. No human participants will be involved in the study.

CB Penny

Dr CB Penny

Chairperson: Human Research Ethics Committee (Medical)

Copy – HREC (Medical) Secretariat: Ms Zanele Ndlovu, Ms Mapula Ramaila and Mr Rhulani Mkansi